BBA - Molecular Cell Research 1873 (2026) 120092

Contents lists available at ScienceDirect

BBA - Molecular Cell Research

journal homepage: www.elsevier.com/locate/bbamcr

Research paper

# Osteocyte transition induced by quiescent vascular smooth muscle cells through paracrine signaling is independent of shear stress

Célio J.C. Fernandes [a], Bram C.J. van der Eerden [b], Rodrigo A. Foganholi Silva [c,d], Gwenny M. Fuhler [e], Maikel P. Peppelenbosch [e], Willian F. Zambuzzi [a,*]

[a] Bioassays and Cell Dynamics Lab, Dept. of Chemistry and Biochemistry, Bioscience Institute, UNESP, Botucatu, 18603-100, Sao Paulo, Brazil
[b] Department of Internal Medicine, Erasmus MC, University Medical Center Rotterdam, Room Ee514, Dr Molewaterplein 40, 3015 GD, Rotterdam, the Netherlands
[c] School of Dentistry, University of Taubaté, 12020-340, Taubaté, São Paulo, Brazil
[d] CEEpiRG - Center for Epigenetic Study and Genic Regulation, Program in Environmental and Experimental Pathology, Paulista University, São Paulo, SP, Brazil
[e] Department of Gastroenterology and Hepatology, Erasmus MC, University Medical Center Rotterdam, 's Gravendijkwal 230, NL-3015 CE, Rotterdam, the Netherlands

ARTICLE INFO

*Keywords:*
Osteoblast
Osteocyte
Small extracellular vesicles
Vascular smooth muscle cells
Shear stress
RANKL

ABSTRACT

We investigated how vascular smooth muscle cells (VSMCs) shape osteolineage fate under mechanosignaling, with emphasis on validating effects in mesenchymal stromal cells (MSCs), a more primitive stage than differentiated osteoblasts. Conditioned media from shear-stressed and non-stressed VSMCs challenged primary human osteoblasts and human MSCs for up to 28 days. Across both cell types, VSMCs robustly promoted osteoblast-to-osteocyte plasticity, evidenced by morphological remodeling and increased expression of osteocyte markers (GP38, SOST, DMP1, miR-23a, FGF23). Notably, non-stressed VSMC–conditioned medium elicited stronger osteocyte-function signatures, including a > 10-fold rise in RANKL transcripts, and these responses were recapitulated in MSCs, demonstrating that VSMC cues instruct osteogenic commitment at an earlier lineage stage and converge on an osteocyte-like phenotype. Mechanistically, small extracellular vesicles (sEVs) emerged as key mediators of VSMC–bone crosstalk: sEV cargo from non-stressed VSMCs displayed higher SOST and DMP1 transcripts, along with phosphor - β-catenin, phospho-connexin-43, and ATP, suggesting pathways that support osteocyte survival and function. Collectively, our data position VSMCs as pivotal instructors of osteolineage progression - from MSC commitment to osteocyte specification - via sEV-dependent communication, with non-stressed VSMCs exerting the strongest effect, particularly on functional readouts such as RANKL. Further, these findings support VSMC-sEV–inspired, cell-free approaches to modulate osteocytogenesis and regulate bone remodeling, while proposing SOST/DMP1/miR-23a as candidate circulating markers of osteocyte function and treatment response.

## 1. Introduction

Bone remodeling and angiogenesis are integral biological processes crucial for bone remodeling and homeostasis [1,2]. Over the last few years, these processes have been closely associated during osteogenesis. Endochondral ossification necessitates the well-coordinated replacement of cartilage by de novo bone deposition. Chondrocytes and bone-differentiating cells cooperate with the capillary network, predominantly coordinated by vascular endothelial growth factor (VEGF) signaling [3–5]. This intricate crosstalk between bone cells and the vascular circuit has been extensively explored, particularly in the context of bone fracture repair and regeneration [6–9].

Osteoblasts, derived from mesenchymal stem cells, continually respond to the bone microenvironment, integrating signals that orchestrate bone remodeling. The regulatory dynamics of this process define the mechanism of osteoblast differentiation, transforming them into bone matrix-producing cells capable of becoming either bone lining cells or pre-osteocytes. In turn, osteocytes, which constitute 90–95 % of specialized bone cells, play a pivotal role by secreting anti-mineralizing molecules like osteocalcin to maintain the surrounding osteoid matrix. Although the biology of osteocytes remains unclear, better comprehension of their biology is crucial for understanding bone disorders due to the dominance of these cells in specialized bone cell populations [10].

Osteocytogenesis is primarily governed by the expression of specific

* Corresponding author.
*E-mail address:* w.zambuzzi@unesp.br (W.F. Zambuzzi).

https://doi.org/10.1016/j.bbamcr.2025.120092
Received 10 July 2024; Received in revised form 10 November 2025; Accepted 3 December 2025
Available online 5 December 2025

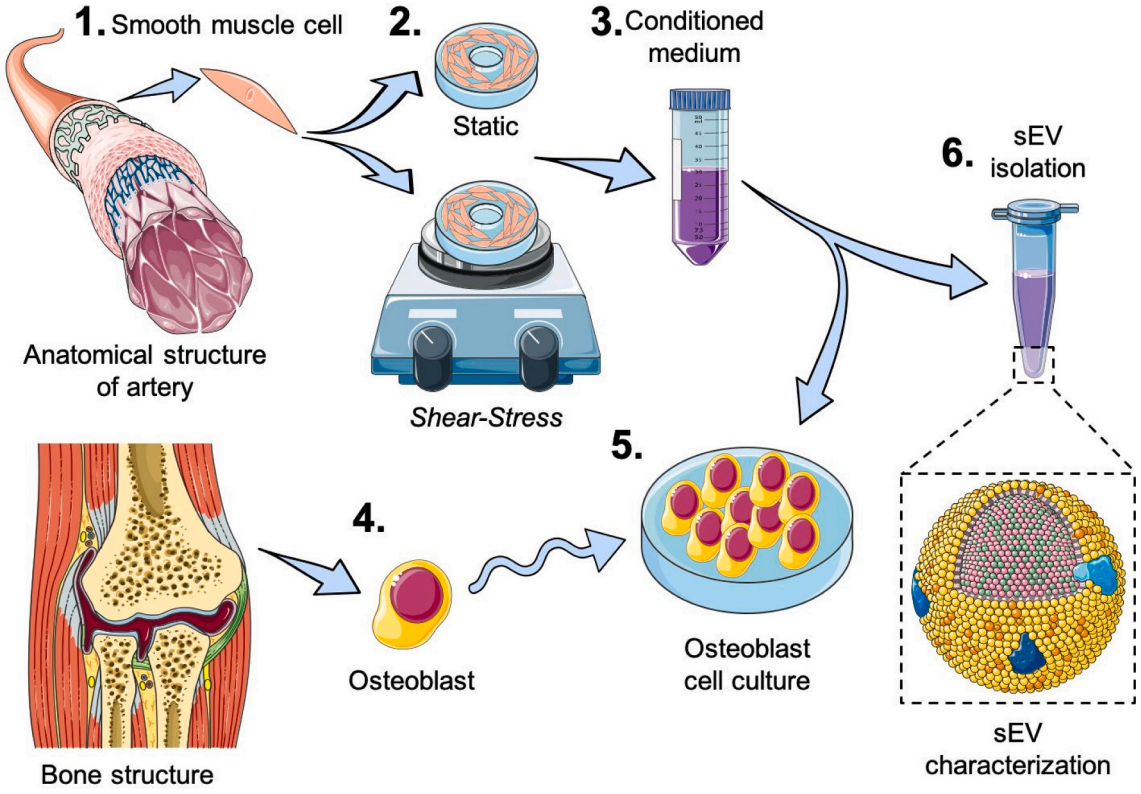


**Fig. 1. Schematic representation of the experimental design used in this study.** Vascular smooth muscle cells (VSMCs) were cultured under static (quiescent) conditions or exposed to mechanical shear stress. The resulting conditioned medium was collected and subjected to kit steps to obtain small extracellular vesicles (sEVs). Osteoblast were then treated with either VSMC-derived conditioned media, allowing the evaluation of paracrine effects on osteogenic commitment, osteoblastic differentiation, and the osteoblast-to-osteocyte transition.

genes that collectively dictate osteocyte morphology and function. Key proteins, such as E11/GP38, contribute to the characteristic star-shaped cell morphology with numerous cytoplasmic processes connecting osteocytes through connexin 43, which also facilitates communication and survival signaling. Additionally, Fibroblast Growth Factor 23 (FGF23) [11–15] and Dentin Matrix Protein 1 (DMP1) play critical roles in mineral homeostasis within bone. Notably, osteocytes emerge as the primary source of RANKL in vertebrates [16–22], a regulator of osteoclastogenesis and subsequent bone remodeling [23,24].

Despite progress in understanding osteocyte biology, limited knowledge of osteocyte ontogeny persists, potentially due to their embedded localization within compact bone tissue and technical challenges in their extraction. Accordingly, our focus has shifted towards investigating in vitro approaches to delineate preliminary events involving bone cells, initially exploring interactions of osteoblasts with biomaterials and, more recently, probing interactions between bone and vascular cells. Our recent work has extensively explored the impact of endothelial and vascular smooth muscle cells (VSMCs) on osteoblasts, revealing the noteworthy contribution of VSMCs to osteoblast-to-osteocyte plasticity [25] and requiring HIF1α [44]. Recognizing the significance of mechanosignaling and forces in bone health, we have delved into the effects of subjecting VSMCs to in vitro shear-stress programs, elucidating the differential mechanisms in osteoblasts responding to shear-stressed or non-stressed VSMCs, particularly in osteocyte ontogeny and function [25].

Altogether, our findings reveal that VSMC–bone communication regulates osteoblast-to-osteocyte transition through sEV-mediated signaling. The strong osteocyte-like response induced by non-stressed VSMC secretomes, including a marked increase in RANKL, underscores a mechanosensitive paracrine axis with translational relevance for bone remodeling and disease.

## 2. Results

### *2.1. VSMC-conditioned medium under shear stress differentially regulates TGFβ/BMP signaling in osteoblasts*

Initially, vascular smooth muscle cells (VSMCs) were cultured under static (quiescent) conditions or exposed to shear stress for up to 72 h. The resulting conditioned media and small extracellular vesicles (sEVs) were collected and subsequently used to treat mesenchymal stromal cells (MSCs) and primary osteoblasts to evaluate paracrine effects on osteogenic differentiation and the osteoblast-to-osteocyte transition (Fig. 1). (See Table 1.)

A significant upregulation of TGFβ1 (Fig. 2a), BMPR2 (Fig. 2c), BMP7 (Fig. 2e), and BMP9 (Fig. 2f) genes was observed in response to shear-stressed VSMCs, with a notable opposite effect on BMP7 in comparison to non-stressed VSMCs (~3-fold higher). TGFβ1 and BMP9 genes were also upregulated in response to conditioned medium from non-stressed VSMCs. Subsequently, the investigation of classical transcription factors RUNX2 (Fig. 1g) and osterix (Fig. 2h), revealed their significant upregulation in groups receiving VSMC-conditioned medium, irrespective of the experimental condition.

To comprehend the activation mechanism of the TGFβ1/BMP signaling pathway stimulus, the involvement of SMAD genes was evaluated. Findings indicated an increase in the expression of SMADs 3 (Fig. S1b), 5 (Fig. S1d), 6 (Fig. S1e), and 7 (Fig. S1f), suggesting a positive involvement of TGFβ/BMP signaling pathways in the osteogenic route promoted in osteoblasts responding to VSMCs. Particularly, the higher expression (~6-fold) of SMAD5 (Fig. S1d) in osteoblasts responding to shear-stressed conditions suggests a loop of autocrine signaling with BMP7 activity (Fig. 2e).

**Table 1**
Primer sequences and PCR cycle conditions.

| Gene | Primer | 5′-3’ Sequence |
|---|---|---|
| BMPr1 | Forward | CATATTAGGCGTGTGCCAAAAA |
| | Reverse | GCTTGTGCTTGCTGTCGTTC |
| BMPr2 | Forward | ATTTGCAGCACAGACGGATATT |
| | Reverse | GACACTGAAAATCTGAGCCTTCT |
| BMP2 | Forward | CCCAGCGTGAAAGAGGAGAC |
| | Reverse | CCATGGTCGACCTTTAGGAG |
| BMP7 | Forward | ACTGTGAGGGGGAGTGTGC |
| | Reverse | CGAAGTAGAGGACGGAGATGG |
| SMAD2 | Forward | GCCGCCAGTTGTGAAGAGAC |
| | Reverse | TGGAGACGACCATCAAGAGACC |
| SMAD3 | Forward | GCTGACACGGAGACACATCG |
| | Reverse | AGCCTCAAAGCCCTGGTTG |
| SMAD4 | Forward | CTTTGAGGGACAGCCATCGT |
| | Reverse | GCCACAGAAATGTTGGGAAA |
| SMAD5 | Forward | GTAAAACGACGGCCAGTTTTCATGGTGAATACTAAGACTGGTTT |
| | Reverse | TTCAATGTAAGCTCACAGTATCTGTACTC |
| SMAD6 | Forward | TACTCTCGGCTGTCTCCTC |
| | Reverse | GAGTTGGTAGCCTCCGTTTC |
| SMAD7 | Forward | GCTGAAACAGGGGGAACGA |
| | Reverse | AGTATGCCACCACGCACCA |
| TGFβ1 | Forward | CAACGAAATCTATGACAAGTTCAAGCAG |
| | Reverse | CTTCTCGGAGCTCTGATGTG |
| RUNX2 | Forward | CCGTCCATCCACTCTACCAC |
| | Reverse | ATGAAATGCTTGGGAACTGC |
| OSTERIX | Forward | CCAGGCAACACTCCTACTCC |
| | Reverse | GCCTTGCCATACACCTTGC |
| RANKL | Forward | AGGGACTCCATCCAAGAAGG |
| | Reverse | GCAGTTTCTGTTCTATTATTCAGGTG |
| SOST | Forward | GCGTTCAAGAATGATGCCACG |
| | Reverse | GCTGTACTCGGACACGTCTTTGG |
| DMP1 | Forward | CAGTGAGGATGAGGCAGACA |
| | Reverse | TCGATCGCTCCTGGTACTCT |
| FGF23 | Forward | TGAGCGTCCTCAGAGCCTAT |
| | Reverse | TTGTGGATCTGCAGGTGGTA |
| FGFr1 | Forward | CTGGGTAGCAACGTGGAGTT |
| | Reverse | ACCATGCAGGAGATGAGGAA |
| FGFr2 | Forward | GGAAAAGAACGGCAGTAAAT |
| | Reverse | GTAGTCTGGGGAAGCTGTAAA |
| FGFr3 | Forward | GGGCTTCTTCCTGTTCATCC |
| | Reverse | AGGGACACCTGTCGCTTGA |
| FGFr4 | Forward | AGATGCTCAAAGACAACGCCT |
| | Reverse | CGCACTTCCACGATCACGTA |
| PTCH | Forward | GGGTCCTCGCTTACAAACTC |
| | Reverse | ATGATGCCATCTGCGTCTAC |
| SUFU | Forward | GAGGGCGAAGTAATTTGTGG |
| | Reverse | AGCCCTCCTTCTGAGTGCTT |
| SHH | Forward | CACCGAGCAGTGGATATGTG |
| | Reverse | AGTGGCCAGGAGTGAAACTG |
| miR23a | Forward | CCGGCTGGGGTTCCTG |
| | Reverse | GGTCGGTTGGAAATCCCTGGC |
| miR17 | Forward | TCAGAATAATGTCAAAGTGCTTACAGTGCAGG |
| | Reverse | GTCACCATAATGCTACAAGTGCCTTCACTC |
| LRP5 | Forward | AAGGGTGCTGTGTACTGGAC |
| | Reverse | AGAAGAGAACTTACGGGAC |
| β-Catenin | Forward | GCGTGGACAATGGCTACTCAAG |
| | Reverse | GTCATTGCATACTGCCCGTCAA |
| GSK3 | Forward | GACTAAGGTCTTCCGACCCC |
| | Reverse | TTAGCATCTGACGCTGCTGT |
| DKK1 | Forward | CCTTGGATGGGTATTCCAGA |
| | Reverse | CCTGAGGCACAGTCTGATGA |
| sFRP1 | Forward | CGGCCAGCGAGTACGACTACGTGAGC |
| | Reverse | GCATCTCGGGCCAGATAGAAGCCGAAG |
| sFRP2 | Forward | CTCGCTGCTGCTGCTCTTC |
| | Reverse | GGCTTCACATACCTTTGGAG |
| CD9 | Forward | TTTAAAAGTGCAGCCGGAGA |
| | Reverse | GCGCCGATGATGTGGAATTT |
| CD63 | Forward | TGATGCCGTGGAAAGCAGAT |
| | Reverse | AGTCAAGCGTCTCGTGGAAG |
| CD81 | Forward | GCGGTGGAAGGAGGAATGAA |
| | Reverse | AGCCCCCTGGATTATGGTCT |
| Fetuin A | Forward | GAATTCCCCGCTCATCCTGTTCT |
| | Reverse | CGTGGAAATCGCAGTCTCCT |
| TNAP | Forward | TTTATAAGGCGGCGGGGGTG |
| | Reverse | AGCCCAGAGATGCAATCGAC |

(*continued on next page*)

**Table 1** (*continued*)

| Gene | Primer | 5′-3’ Sequence |
|---|---|---|
| NPP1 | Forward | TTTGCCGATTGAGGATTTTC |
| | Reverse | CCACTGACGACATTGACACC |
| SMPD3 | Forward | GCCTATCACTGTTACCCCAAC |
| | Reverse | GACGATTCTTTGGTCCTGAGG |
| GP38 | Forward | GGGAACGATGTGGAAGGTGT |
| | Reverse | GCTCTTTAGGGCGAGTACCT |
| VEGF | Forward | TGCAGATTATGCGGATCAAACC |
| | Reverse | TGCATTCACATTTGTTGTGCTGTAG |
| VEGFr | Forward | CAGGCCCAGTTTCTGCCATT |
| | Reverse | TTCCAGCTCAGCGTGGTCGTA |
| Notch1 | Forward | GGAAGTGTGAAGCGGCCAATG |
| | Reverse | ATAGTCTGCCACGCCTCTGC |
| Notch2 | Forward | TGTCGAGATGGCTATGAACCCTG |
| | Reverse | GCAGCGGTTCTTCTCACAGG |
| Nocth3 | Forward | TGTCTGCCAGAGTTCAGTGGTG |
| | Reverse | AGGAGCAGAGGAAGCGTCCATC |
| Notch4 | Forward | TTGTCCTCCCTCCTTCTGTTCC |
| | Reverse | AGAAGTCCCGAAGCTGGCAC |
| Jag1 | Forward | TGCCTCTGTGAGACCAACTG |
| | Reverse | GTTGGGTCCTGAATACCCCT |
| Jag2 | Forward | GTGGCAAGAACTGCTCCGTG |
| | Reverse | TGCCTCTGTGAGACCAACTG |
| BMP9 | Forward | AGAACGTGAAGGTGGATTTCC |
| | Reverse | CGCACAATGTTGG ACGCTG |
| HIF1α | Forward | CATAAAGTCTGCAACATGGAAGGT |
| | Reverse | ATTTGATGGGTGAGGAATGGGTT |
| HIF1β | Forward | CAAGCCCCTTGAGAAGTCAG |
| | Reverse | GAGGGGCTAGGCCACTATTC |
| Integrin β1 | Forward | GCCGCGCGGAAAAGATGAA |
| | Reverse | TGCTGTTCCTTTGCTACGGT |
| Src | Forward | CAACACAGAGGGAGACTGGT |
| | Reverse | AGCTTCTTCATGACCTGGGC |
| FAK | Forward | TCAGCTCAGCACAATCCTGG |
| | Reverse | CTGAAGCTTGACACCCTCGT |
| Cofilin | Forward | TGTGCGGCTCCTACTAAACG |
| | Reverse | TCCTTGACCTCCTCGTAGCA |
| AKT | Forward | CAGCGCGGCCCGAAGGAC |
| | Reverse | GACGCTACAGCGCTCCTCTC |
| ERK | Forward | AACAGGCTCTGGCCCACCCAT |
| | Reverse | GCAGCGCCTCCCTTGCTAGA |
| JNK | Forward | AAAGGTGGTGTTTTGTTCCCAGGT |
| | Reverse | TGATGATGGATGCTGAGAGCCATTG |
| p38 | Forward | GAGAACTGCGGTTACTTA |
| | Reverse | ATGGGTCACCAGATACACAT |
| GAPDH | Forward | GACTCATGACCACAGTCCATGC |
| | Reverse | AGAGGCAGGGATGATGTTCTG |

### *2.2. VSMC-derived paracrine signaling drives osteoblast plasticity towards osteocytes under shear and static conditions*

Osteoblasts were assessed for changes in morphology in response to both shear-stressed and non-stressed VSMCs. Osteoblasts displayed cytoplasmic projections resembling osteocyte-related morphology (Fig. 3a) when exposed to conditioned medium from VSMCs, inducing an osteocyte-like appearance. While the number of osteocyte-like cells (Fig. 3b) did not show significant differences between both conditions, this data reinforced earlier findings indicating osteoblast-to-osteocyte transition in response to VSMCs.

Further addressing classical molecular biomarkers of osteocytes, VSMCs strongly stimulated osteocytogenesis in vitro, as evidenced by elevated expression of mir-23a (Fig. 3c), DMP1 (Fig. 3d), SOST (Fig. 3e), FGF23 (Fig. 3f), and GP38 (Fig. 3g), regardless of shear stress.

Subsequently, other functional biomarkers in osteocytes were investigated. Genes related to the FGFR family showed differential expression, with FGFR1 downregulated (Fig. 4a), while FGFR2 (Fig. 4b; ~2-fold), FGFR3 (Fig. 4c; ~5-fold), and FGFR4 (Fig. 4d; ~15-fold) genes were upregulated. The Shh signaling pathway was also explored, revealing increased expression of Shh (Fig. 4e; ~7-fold), Ptch1 (Fig. 4f; ~10-fold), and SUFU (Fig. 4g; ~3-fold). Notably, a significant increase in RANKL expression was observed in response to the non-stressed VSMCs stimulus (Fig. 4h; ~10-fold), validating the functional performance of differentiated osteocytes obtained in response to VSMCs paracrine signaling.

### *2.3. Possible mechanism involving small extracellular vesicles in VSMCs-induced osteocytogenesis*

Suggesting that VSMCs release molecules that trigger signaling pathways for osteoblast plasticity, we hypothesized the involvement of extracellular vesicles (EVs) in the crosstalk between VSMCs and osteoblasts. EVs were isolated from VSMC-conditioned medium, revealing a significant involvement of tetraspanins (CD9 and CD81) in both shear-stressed and non-stressed VSMCs (Fig. 5a-b), while CD63 was significantly higher in non-stressed conditions (Fig. 5c), as confirmed by fluorescence microscopy (Fig. 5d). Flow cytometry further confirmed the presence of CD9, CD63, and CD81 in these cells (Fig. 5e-f).

A specific analysis of sEV was conducted using Nano Tracking Analysis (NTA) and Transmission Electron Microscopy. sEV, approximately 140 nm in diameter (Fig. 6a-f), exhibited higher concentrations in shear-stressed VSMCs compared to non-stressed VSMCs. Additionally, the expression of SMPD3, an important marker of vesicle biogenesis, supported these findings (Fig. 6 g-h, j). The charge on the sEV membrane, indicating their capacity to interact with the membrane of target cells, was also evaluated (Fig. 6i).

Following the osteoblast analyses described above, we sought to

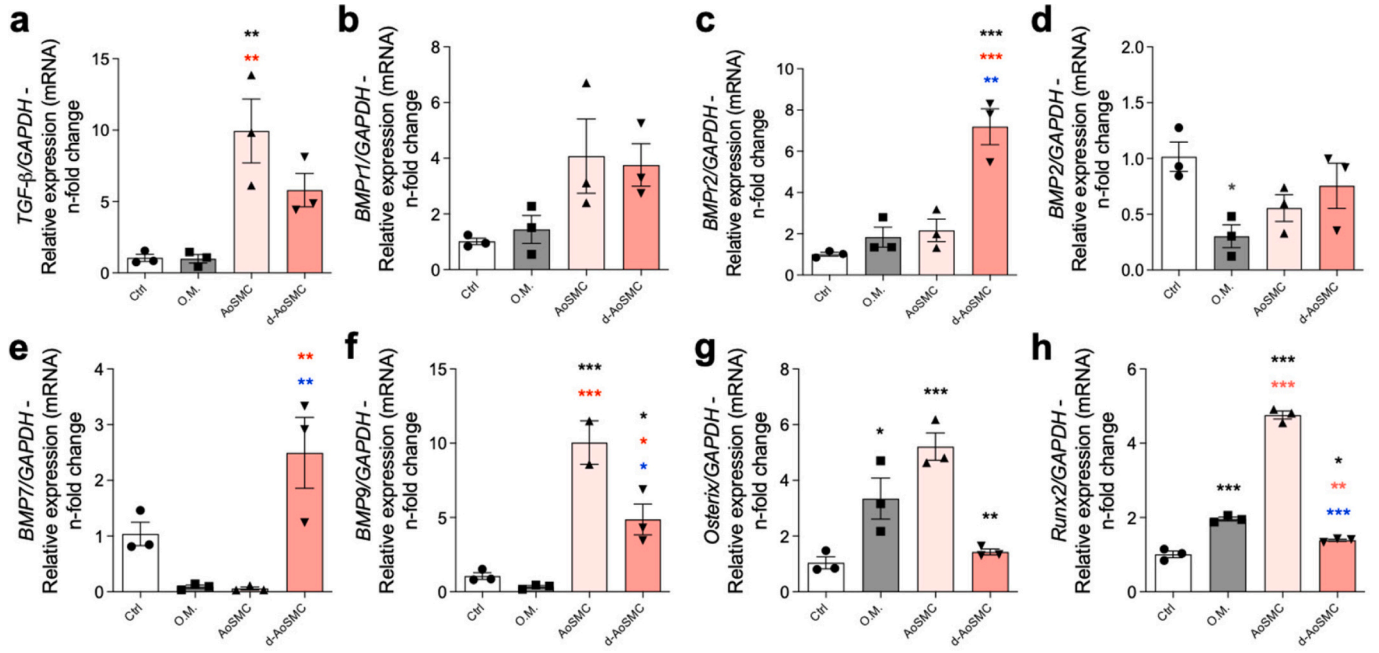


**Fig. 2. VSMCs elicit expression of osteogenic gene markers in osteoblasts.** Following 28 days in culture, in response to shear-stressed (d-AoSMC) and non-stressed (AoSMC) VSMCs conditioned media, cells were harvested in TRIzol for mRNA extraction. Osteogenic gene markers were evaluated, including: **(a)** TGFβ, **(b)** BMPr1, **(c)** BMPr2, **(d)** BMP2, **(e)** BMP7, **(f)** BMP9, **(g)** Osterix, and **(h)** RUNX2. The impact of VSMCs on osteoblasts was compared with control groups: Ctrl - cultures maintained under routine conditions, and O.M. - cultures treated with classical chemical osteostimulation medium. The graphs depict the analysis of 3 independent replicates. qPCR data were normalized using GADPH as a housekeeping gene. Statistics: $*p < 0.05$; $**p < 0.1906$, $***p < 0.0002$: Significant statistical difference when compared to Ctrl. $*p < 0.05$; $**p < 0.1906$; $***p < 0.0002$: Statistical difference when compared with the O.M.. $*p < 0.05$; $**p < 0.1906$; $***p < 0.0002$: Statistical difference when comparing shear-stressed (d-AoSMC) and non-stressed (AoSMC) VSMCs. Note: $n = 3$ independent biological replicates. Each condition was analyzed in technical triplicate, and the technical triplicates corresponding to each biological replicate were pooled prior to performing the PCR reaction.

determine whether VSMC-derived cues also operate at an earlier osteolineage stage; therefore, we validated these effects in mesenchymal stromal cells (MSCs), which represent a more primitive, pre-commitment state. Treatment of MSCs with small extracellular vesicles (sEVs) from primary aortic smooth muscle cells (AoSMCs) induced significant changes in osteocytic gene expression (Fig. 7). SOST and DMP1 transcripts were markedly increased in MSCs exposed to sEVs from shear-stressed AoSMCs (d-AoSMC) compared with untreated controls, osteogenic medium (O.M.), and sEVs from non-stressed AoSMCs. In contrast, FGF23 expression remained stable across groups. Regarding microRNA regulation, miR-23a was significantly increased by sEVs from non-stressed AoSMCs, whereas sEVs from d-AoSMCs induced a modest but significant reduction relative to AoSMC-derived sEVs. Taken together, these findings indicate that the mechanical status of the donor VSMCs imprints distinct osteocytogenic signals on MSCs: shear-derived sEVs selectively upregulate late osteocyte markers (SOST, DMP1), while differentially modulating miR-23a expression (Fig. 7).

### 2.4. Small extracellular vesicle (sEV) cargo profiling and signaling

Following the robust osteocytogenic responses observed in osteoblasts and MSCs, we next interrogated the cargo of VSMC-derived small extracellular vesicles (sEVs). sEVs from non-stressed aortic smooth muscle cells (AoSMCs) contained higher transcript levels of DMP1, SOST (≈100-fold), and FGF23 than sEVs from shear-stressed AoSMCs (d-AoSMCs) (Fig. 8a–d). Canonical sEV markers (CD9, CD63, CD81) and SMPD3 confirmed vesicle identity (Fig. 8e–h). To assess protein cargo, we quantified SOST in the isolated sEV fraction and in unfractionated conditioned medium (CM). In both readouts, preparations from non-stressed AoSMCs displayed greater SOST content than those from d-AoSMCs (Fig. 8i,j), consistent with the mRNA data and indicating enrichment of SOST at both transcript and protein levels. Pathway analysis supported the involvement of Notch and Wnt/β-catenin signaling: sEVs carried the Notch ligands Jagged1 and Jagged2 (Fig. 9), as well as phosphorylated β-catenin and phosphorylated connexin-43 (Fig. 10b–c). Recipient, differentiated osteocytes exhibited high β-catenin levels under both conditions (Fig. 10d–g). An overview of additional Notch and Wnt/β-catenin components is shown in Fig. S2.

### 2.5. MMP2 activity and ATP-enriched sEVs support osteocyte differentiation

High-profile activity of Collagen1a1 and MMP2 genes (Fig. 11a-b, respectively) was observed, while MMP9 was significantly down-regulated (Fig. 11c). Despite elevated levels of TIMP1 (Fig. 11d), TIMP2 (Fig. 11e), and RECK (Fig. 11f), increased MMP2 activity was noted (Fig. 11g-i) as measured by zymography technology. Genes related to cell adhesion (Integrin-β3, FAK, Src, Cofilin) were highly expressed in differentiated osteocytes (Fig. S3a-d). Investigation into ATP levels in pooled sEV revealed that VSMCs-released sEV carried high levels of ATP in both culture conditions (Fig. 12a). Genes related to mineral homeostasis (Fetuin-A, NPP1, TNAP) and classical markers (ALP, BSP, osteocalcin, osteopontin) were positively regulated in differentiated osteocytes (Fig. 12b-h). Additionally, we evaluated the gene expression of NPP1 and TNAP in both vascular smooth muscle cells (VSMCs) subjected or not to shear stress and their respective small extracellular vesicles (sEVs). As shown in Fig. S4, no significant differences were observed in the transcript levels of NPP1 (Fig. S4a,c) and TNAP (Fig. S4b,d).

## 3. Discussion

This study provides novel insight into the contribution of vascular smooth muscle cells (VSMCs) to osteoblast-to-osteocyte transition

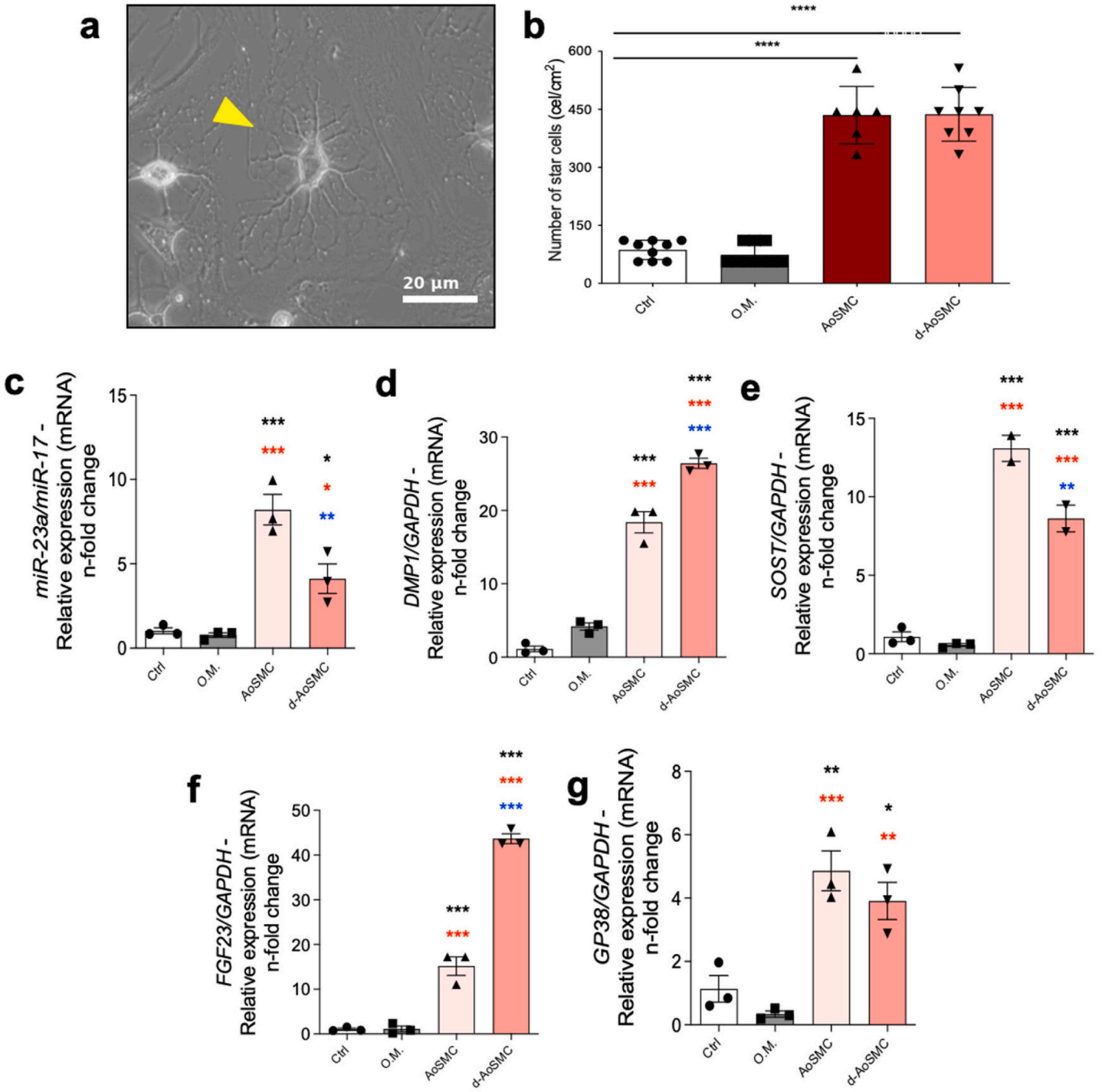


**Fig. 3. VSMC paracrine signaling induces osteoblast-to-osteocyte plasticity under shear and static conditions.** Following 28 days in culture, cells responded to shear-stressed (d-AoSMC) and non-stressed (AoSMC) VSMCs conditioned media. Cell morphology was analyzed using light optical microscopy **(a)**, and the number of star-shaped cells was quantified **(b)**. Simultaneously, cells were harvested in TRIzol for mRNA extraction, and subsequent analysis of osteocyte-related genes was performed to confirm the phenotype, including miR-23a **(c)**, DMP1 **(d)**, SOST **(e)**, FGF23 **(f)**, and GP38 **(g)**. The impact of VSMCs on osteoblasts was compared with control groups: Ctrl - cultures maintained under routine conditions, and O.M. - cultures treated with classical chemical osteostimulation medium. The graphs represent the analysis of 3 independent replicates. qPCR data were normalized using GADPH as a housekeeping gene, and miR-17 was used to normalize the data of miR-23a expression. Statistics: $*p < 0.05$; $**p < 0.1906$, $***p < 0.0002$; $****p < 0.0001$: Significant statistical difference when compared to Ctrl. $*p < 0.05$; $***p < 0.0002$: Statistical difference when compared with the O.M.. $**p < 0.1906$; $***p < 0.0002$: Statistical difference when comparing osteoblasts cultures responding to shear-stressed (d-AoSMC) and non-stressed (AoSMC) VSMCs. Note: $n = 3$ independent biological replicates. Each condition was analyzed in technical triplicate, and the technical triplicates corresponding to each biological replicate were pooled prior to performing the PCR reaction.

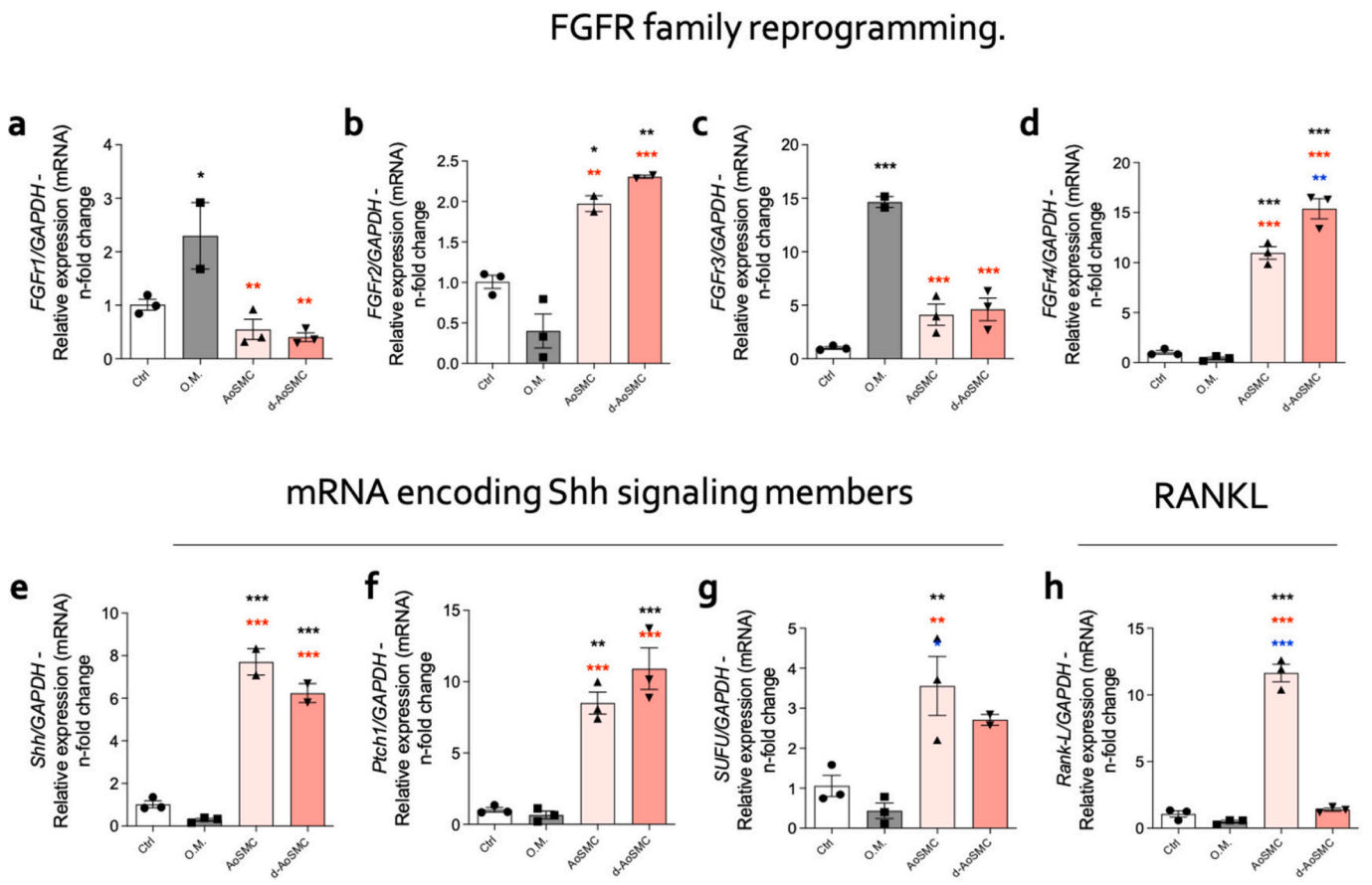


**Fig. 4. Genes related to osteocyte function: RANKL gene is reprogrammed in response to non-stressed VSMCs.** Following 28 days in culture responding to shear-stressed (d-AoSMC) and non-stressed (AoSMC) VSMCs conditioned media, cells were harvested in TRIzol for mRNA extraction and subsequent qPCR analysis. Osteocyte gene markers were evaluated, including **(a)** FGFR1, **(b)** FGFR2, **(c)** FGFR3, **(d)** FGFR4, **(e)** SHH, **(f)** PTCH1, **(g)** SUFU, and **(h)** RANKL. The impact of VSMCs on osteoblasts was compared with control groups: Ctrl - cultures maintained under routine conditions, and O.M. - cultures treated with classical chemical osteostimulation medium. The graphs represent the analysis of 3 independent replicates. qPCR data were normalized using GADPH as a housekeeping gene. Statistics: $*p < 0.05$; $**p < 0.1906$, $***p < 0.0002$: Significant statistical difference when compared to Ctrl. ***p < 0.0002: Statistical difference when compared with the O.M.. *p < 0.05; **p < 0.1906; ***p < 0.0002: Statistical difference when comparing shear-stressed (d-AoSMC) and non-stressed (AoSMC) VSMCs. Note: $n = 3$ independent biological replicates. Each condition was analyzed in technical triplicate, and the technical triplicates corresponding to each biological replicate were pooled prior to performing the PCR reaction.

through paracrine signaling pathways that are, to a large extent, independent of mechanical stimulation. Osteocytes play a crucial role in bone remodeling, being the primary postnatal source of sclerostin and RANKL, two regulators of osteoblast and osteoclast function in vertebrates [26,27]. By employing conditioned media derived from both shear-stressed and non-stressed (quiescent) VSMCs, we observed distinct phenotypic and molecular changes in primary osteoblasts that support the concept of VSMC-mediated modulation of osteoblast plasticity.

A key finding is the greater osteogenic and osteocytic differentiation potential of conditioned medium from non-stressed VSMCs, suggesting that shear stress is not required for, and may even modulate, the release of osteoinductive signals by these cells. Morphological changes consistent with osteocyte-like phenotypes, as well as the robust upregulation of hallmark osteocyte genes such as DMP1, SOST, FGF23, GP38, and miR-23a [28,29], were more pronounced in the group treated with medium from quiescent VSMCs. Moreover, RANKL, a functional marker of mature osteocytes, was increased by more than 10-fold under the same condition, highlighting the enhanced osteocytic function driven by non-stressed VSMCs. Extending these analyses to mesenchymal stromal cells (MSCs), a pre-commitment, highly plastic stage in the osteolineage, demonstrated that VSMC-derived cues act upstream of osteoblast differentiation, imposing an osteogenic/osteocytic program already at this undifferentiated state. In MSCs, sEVs from shear-stressed donors preferentially increased late osteocyte markers (SOST, DMP1), whereas the mechanical status of the donor differentially modulated miR-23a, indicating stage-specific decoding of VSMC paracrine signals across early (MSC) and later (osteoblast) stages. Additionally, we observed that isolated vesicles, when used to treat mesenchymal cells, have the ability to differentially modulate genes involved in the regulation of the osteoblast-to-osteocyte transition, including DMP1, SOST, and miR-23a.

Nonetheless, we also identified genes whose expression was significantly modulated by shear stress, highlighting the complexity of VSMC signaling. SMAD5, a key transducer of BMP signaling [30], was notably upregulated in osteoblasts treated with shear-stressed VSMC media, along with variable regulation of BMP7, FGFRs, and SHH components. These findings suggest that although mechanical stimuli modulate secretome composition, they are not strictly required to induce the osteoblast-to-osteocyte transition. Consistent with this notion, our validation in MSCs indicates that VSMC-derived cues can impose osteogenic/osteocytic programs already at an undifferentiated stage, with donor mechanical status shaping marker selection and magnitude.

From a physiological perspective, it is relevant to consider that bone vasculature is uniquely adapted to low-flow, low-shear environments. Ramasamy et al. demonstrated that bone-specific vessels, particularly sinusoidal capillaries in the metaphysis, experience markedly reduced shear stress compared with other vascular beds [31]. Quiescent VSMCs maintained under static conditions may thus more accurately reflect the native hemodynamic environment of the bone microvasculature.

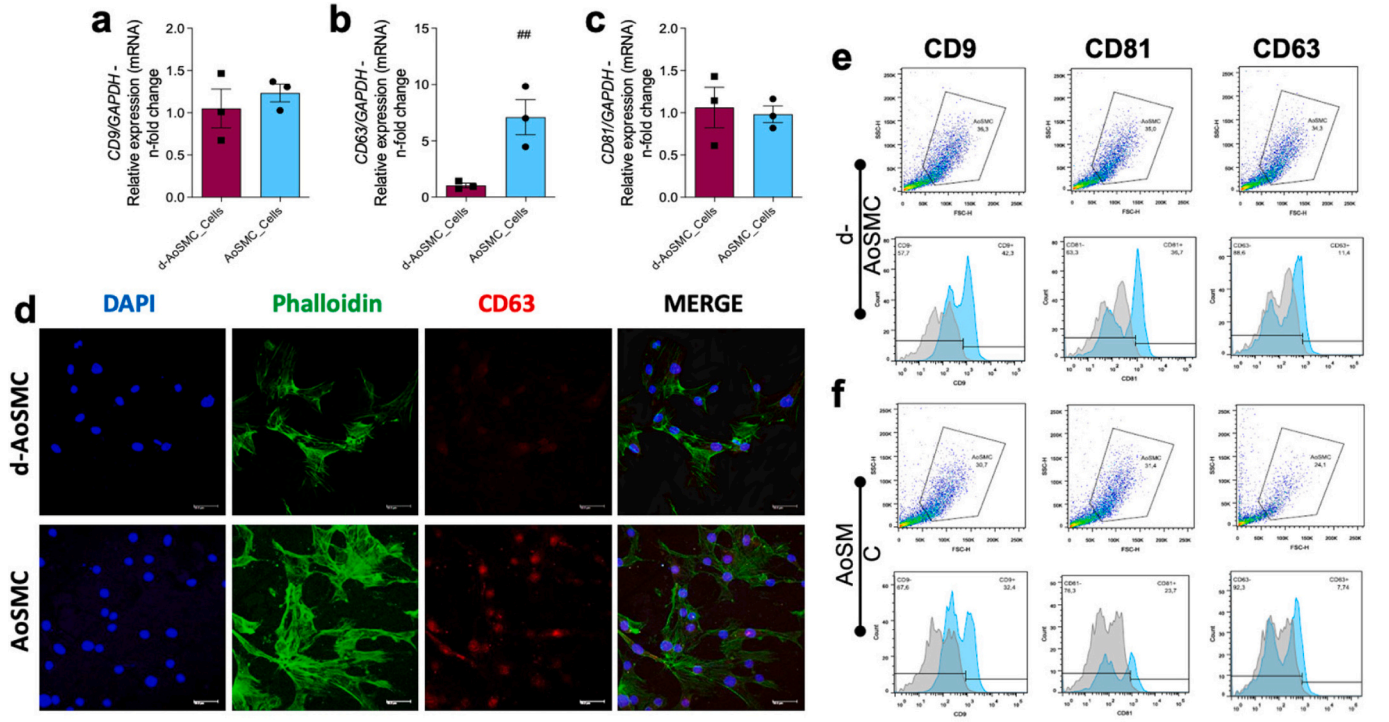


**Fig. 5. VSMCs maintain the expression of sEV biomarkers.** After 3 days of culture, cells were collected in TRIzol to analyze the expression of Tetraspanins CD9 **(a)**, CD63 **(b)**, and CD81 **(c)**. Cells grown on coverslips were labeled with a CD63-specific antibody and analyzed using laser confocal microscopy **(d)**. Moreover, the conditioned media were collected, and the extracellular vesicles (EVs) were pooled to analyze the presence of the tetraspanins on their surfaces by FACS technology. The sEV were properly labeled with antibodies anti-CD9, anti-CD63, and anti-CD81 **(e, f)**, considering shear-stressed (d-AoSMC) and non-stressed (AoSMC) VSMCs, respectively. The graphs represent the analysis of 3 independent replicates. qPCR data were normalized using GADPH as a housekeeping gene. Statistics: $\#\#p < 0.1906$: Statistical difference when compared shear-stressed (d-AoSMC) and non-stressed (AoSMC) VSMCs. Note: $n = 3$ independent biological replicates. Each condition was analyzed in technical triplicate, and the technical triplicates corresponding to each biological replicate were pooled prior to performing the PCR reaction.

Furthermore, in their subsequent work, Ramasamy et al. identified type H and type L vessels as critical components in maintaining osteoprogenitor niches and ensuring osteoblast survival and differentiation [32]. These specialized capillaries are functionally distinct from conventional arteries and veins, reinforcing the idea that vascular regulation of bone biology is mediated by finely tuned, tissue-specific signals rather than generalized hemodynamic forces.

The paracrine contribution of VSMCs to osteogenic commitment appears to be mediated in large part by small extracellular vesicles (sEVs) containing regulatory molecules such as mRNAs, miRNAs, ATP, and phosphorylated signaling proteins [33]. These vesicles can influence recipient osteoblasts via non-contact-dependent mechanisms and may contribute to skeletal remodeling at a distance. Pathological states such as Hutchinson-Gilford Progeria Syndrome further support this concept, where systemic vascular dysfunction coincides with profound skeletal abnormalities [34].

Although we observed a strong osteoinductive effect from quiescent VSMCs, certain markers such as SMAD5, DMP1, and FGF23 were also modulated by shear stress, indicating a layered and context-dependent signaling profile. Moreover, qPCR evidence suggested a finely balanced activation of the Wnt/β-catenin pathway, with both agonists (β-catenin, Axin2) and antagonists (DKK1, sFRP) elevated in recipient cells, likely representing a dynamic homeostatic adaptation to vesicle-derived stimuli. Furthermore, we recognized that qPCR only confirms short RNA fragment presence within sEVs; whether full-length transcripts are transferred functionally remains to be demonstrated in future experiments involving reporter systems and imaging. Terminologically, we adopted the recommended MISEV2024 term “sEVs” and clarified the limitations of our isolation protocol. NTA analyses confirmed vesicle heterogeneity, with particle diameters ranging from 50 to 400 nm [35].

Importantly, previous work from our group has shown that fibroblast-derived conditioned media are also capable of modulating osteoblast gene expression, including the upregulation of osteocyte-related markers such as SOST, DMP1, and FGF23 [36]. However, the molecular profile induced by fibroblast secretomes is mechanistically distinct from that triggered by VSMCs. Specifically, fibroblast-conditioned media primarily act through extracellular matrix (ECM) remodeling cues and do not induce the same morphological transition towards an osteocyte-like phenotype, nor do they robustly engage canonical pathways such as Wnt/β-catenin or produce vesicle-mediated delivery of phosphorylated signaling proteins. In contrast, VSMCs, particularly under quiescent conditions, appear to engage a broader and more functionally integrated network involving SHH, MAPK/ERK, and Wnt signaling components, suggesting a cell-type-specific paracrine signature that more directly promotes the osteoblast-to-osteocyte transition.

Collectively, our findings show that VSMCs, especially under quiescent conditions that resemble physiological bone vasculature, promote the osteoblast-to-osteocyte transition via sEV-mediated paracrine signaling (Fig. 13). Crucially, validation in MSCs demonstrates that VSMC cues act upstream of osteoblast commitment: shear-stressed VSMC sEVs preferentially prime naïve MSCs by upregulating late osteocyte markers (e.g., SOST, DMP1), whereas quiescent VSMC secretomes/sEVs maximize osteocyte functional outputs in committed osteoblasts (e.g., robust RANKL induction). This stage-specific decoding of a mechanosensitive vascular signal supports a tissue-specific vascular–skeletal communication axis that operates independently of generalized hemodynamic forces. Strategically, leveraging donor VSMC mechanical state and vesicle cargo composition may enable tuning of osteocyte specification and function for bone repair and skeletal

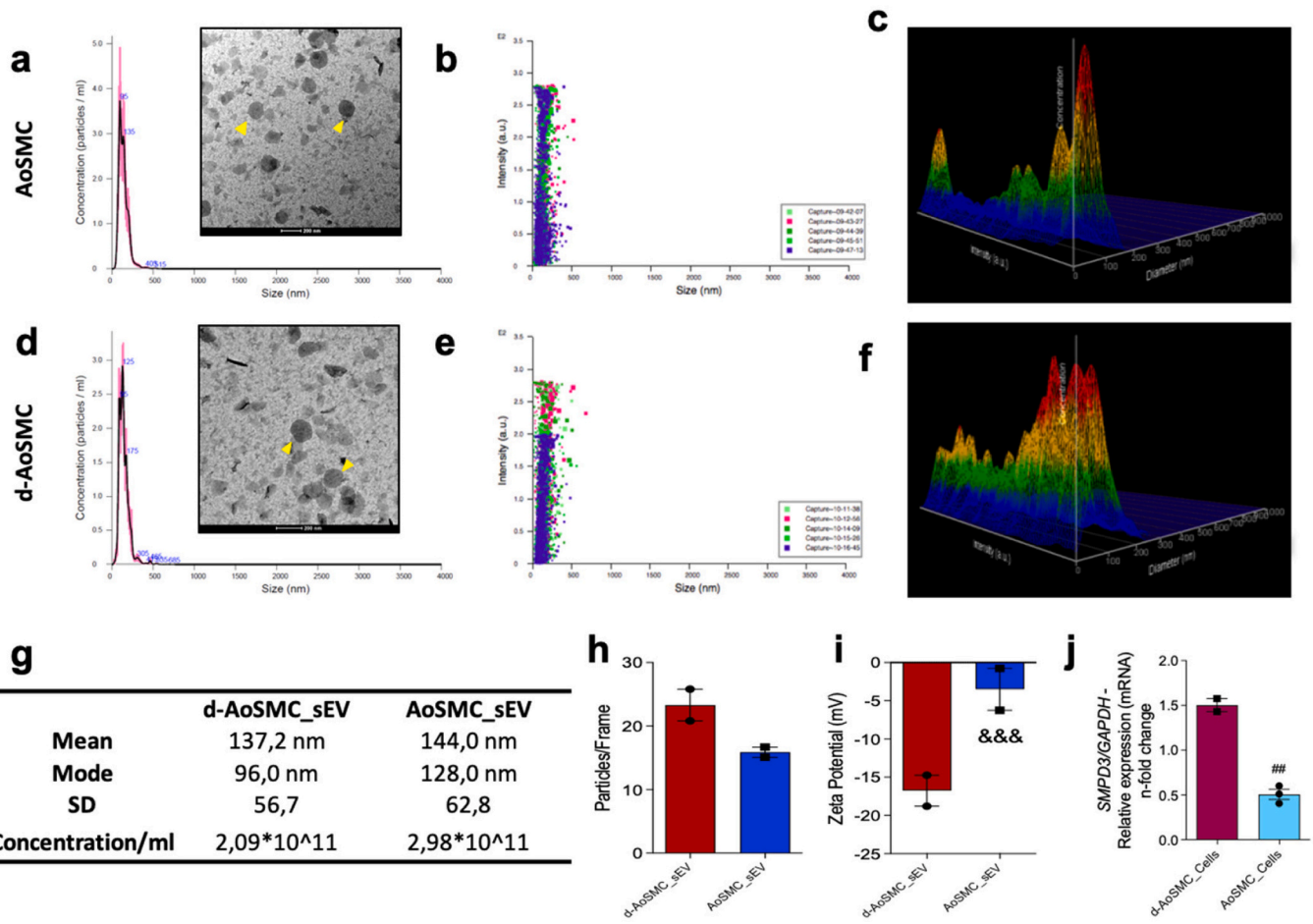


g

| | d-AoSMC_sEV | AoSMC_sEV |
|---|---|---|
| Mean | 137,2 nm | 144,0 nm |
| Mode | 96,0 nm | 128,0 nm |
| SD | 56,7 | 62,8 |
| Concentration/ml | 2,09*10^11 | 2,98*10^11 |




**Fig. 6. sEV characterization reveals differential properties in response to mechanosignaling.** After 3 days of culture, the conditioned media were collected from cultures responding to shear-stressed (d-AoSMC) and non-stressed (AoSMC) VSMCs, and the extracellular vesicles (EVs) were pooled and characterized, as recommended (MISEV, 2018). The EVs were evaluated for size and concentration through Nanoparticle Tracking Analysis (NTA) and Transmission Electron Microscopy **(a-h)**. Additionally, Zeta Potential was also evaluated **(i)**. Cells were also collected to evaluate the gene expression of SMPD3 **(j)**. The graphs represent the analysis of 3 independent replicates. qPCR data were normalized using GADPH as a housekeeping gene. Statistics: $\&\&\&p < 0.0002$: Statistical difference when compared shear-stressed (d-AoSMC) and non-stressed (AoSMC) released sEV. $\#\#p < 0.1906$: Statistical difference when comparing shear-stressed (d-AoSMC) and non-stressed (AoSMC) VSMCs. Note: $n = 3$ independent biological replicates. Each condition was analyzed in technical triplicate, and the technical triplicates corresponding to each biological replicate were pooled prior to performing the PCR reaction.

disorder interventions.

## 4. Methods

### 4.1. Antibodies

The study utilized specific antibodies, each serving a distinct purpose. The antibodies and their respective details are as follows: β-Catenin (6B3) Rabbit mAb #9582, Phospho-β-Catenin (Ser33/37/Thr41) Antibody #9561, Phospho-Connexin 43 (Ser368) Antibody #3511 (Cell Signaling, Danvers, MA, USA), β-Actin Antibody sc-47,778 (Santa Cruz Biotechnology, Dallas, Texas, USA).

### 4.2. Cell culture

Cells were maintained at 37 °C and at 5 % $CO_2$ atmosphere and 95 % humidity. Cells were daily evaluated for morphological variability, color of the culture medium, etc. 1. Osteoblastic cells: For differentiation we used human osteoblasts (HOEL) obtained through joint work with the School of Dentistry of Bauru, FOB-USP, and maintained in our cell bank. During growth, they were maintained and grown in Dulbecco's Modified Eagle Medium (DMEM, Low glucose) containing antibiotics (100 U/mL penicillin, 100 mg/mL streptomycin) and 10 % Bovine Fetal Serum (SFB, Nutricell, Campinas, SP), Brazil). 2. Endothelial Cells: Endothelial cells, HCAEC and HUVEC, were maintained in Endothelial Cell Basal Medium-2 (EBM-2) medium supplemented with 0.5 mL of Epidermal Growth Factor (hEGF), 0.5 mL of Hydrocortisone, 0.5 mL of Gentamicin Sulfate Amphotericin B (GA-1000), 2.0 mL Bovine Brain Extract (BBE), 10 mL Fetal Bovine Serum (FBS), 0.5 mL Ascorbic Acid and antibiotics (100 U/mL penicillin, 100 mg/mL streptomycin). The cells, medium and the trophic factors were obtained together with LONZA; Muscle Cells: Already the smooth muscle cell of aortic origin was maintained in adequate medium - Smooth Muscle Cell Basal Medium (SmBM) supplemented with 0.5 mL Insulin, 1.0 mL Human Fibroblast Growth Factor B (hFGF-B), 0.5 mL Gentamicin Sulfate Amphotericin B (GA-1000), 25 mL Fetal Bovine Serum (FBS), 0.5 mL Epidermal Growth Factor (hEGF) and antibiotics (100 U/mL penicillin, 100 mg/mL streptomycin). Cells and factors were obtained along with LONZA.

### 4.3. Mesenchymal stromal cells (MSCs)

To better evaluating osteogenic differentiation from an undifferentiated stem cell, we have used MSC, which were maintained and grown in Dulbecco's Modified Eagle Medium (DMEM) containing antibiotics (100 U/mL penicillin, 100 mg/mL streptomycin) and 10 % Bovine Fetal Serum (SFB). The cells were maintained in culture for 28 days and

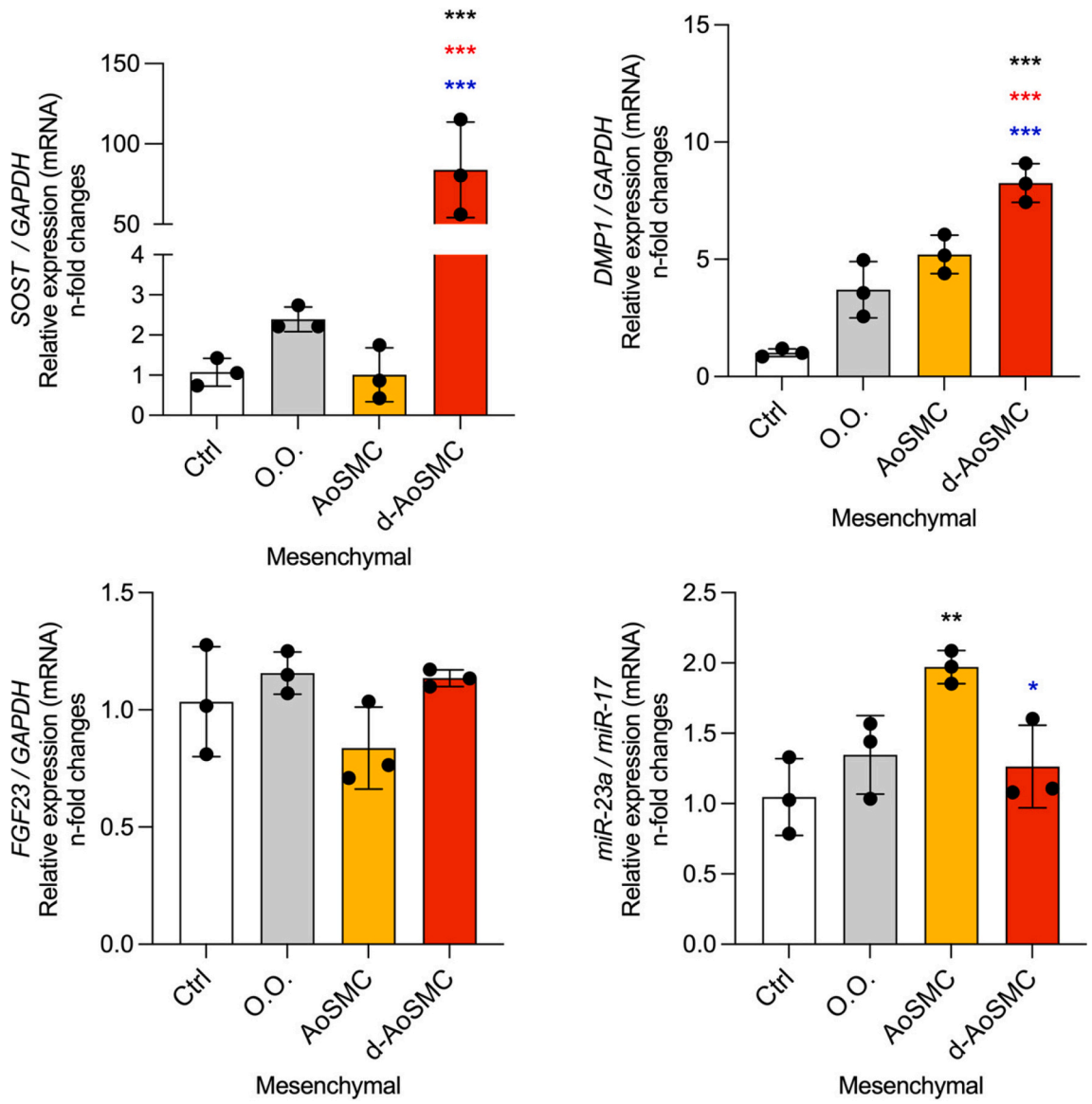


**Fig. 7. sEV modulate the expression of osteocyte markers in MSCs.** Mesenchymal stromal cells (MSCs) were treated for 28 days with sEVs derived from primary smooth muscle cells (AoSMC). After treatment, cells were collected in TRIzol for RNA extraction, cDNA synthesis, and gene expression analysis of SOST, DMP1, FGF23, and miR-23a. Expression values were normalized to GAPDH or miR-17 as reference genes. **$p < 0.1906$, ***$p < 0.0002$: Significant statistical difference when compared to control. ***$p < 0.0002$: Statistical difference when compared with the Osteogenic Medium. *$p < 0.05$, ***$p < 0.0002$: Statistical difference when compared with the AoSMC treatment. Note: $n = 3$ independent biological replicates. Each condition was analyzed in technical triplicate, and the technical triplicates corresponding to each biological replicate were pooled prior to performing the PCR reaction.

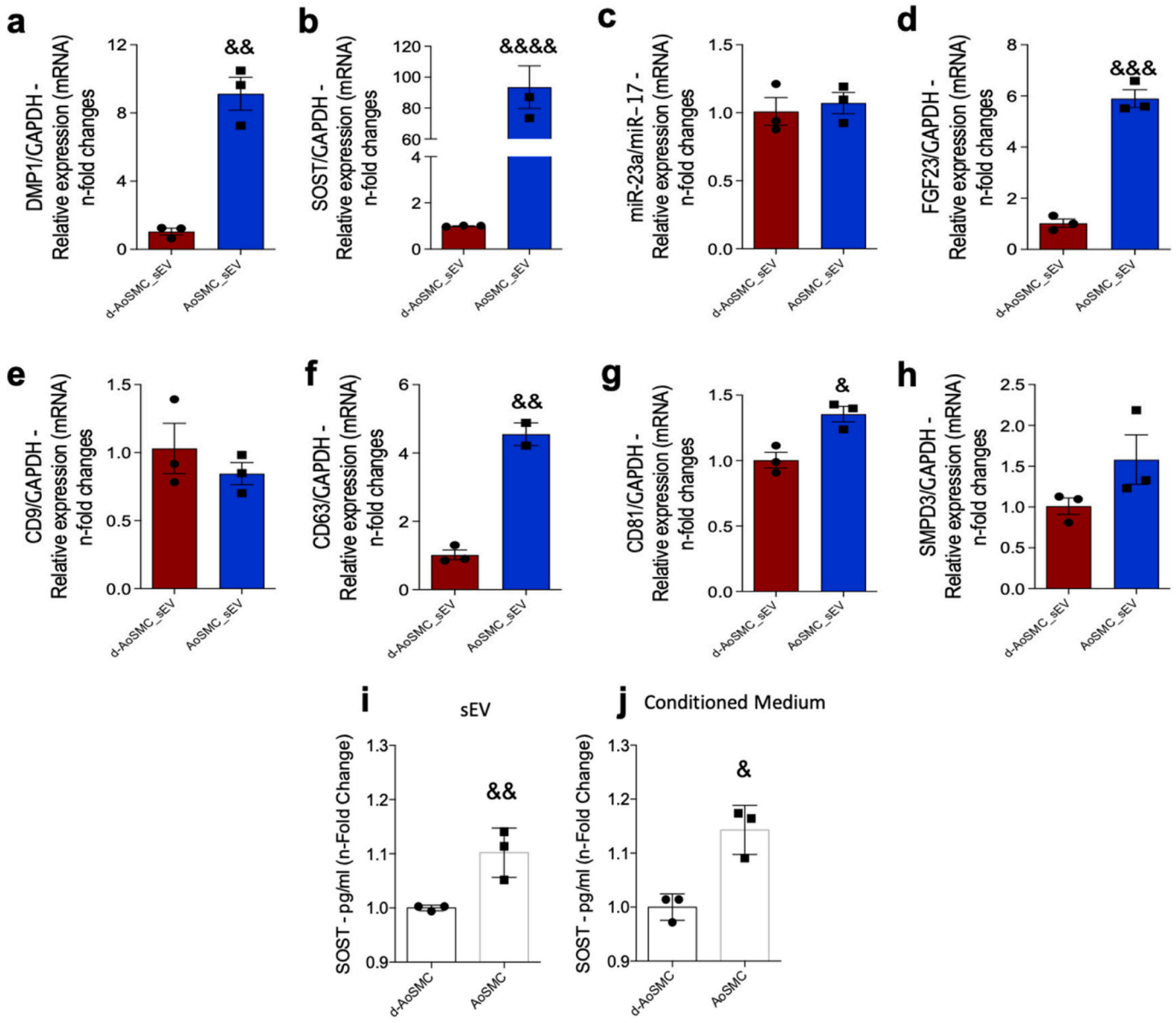


**Fig. 8. Mechanosignaling differentially packages osteocyte-related mRNAs into VSMC-derived sEV cargo.** After 3 days in culture, conditioned media from shear-stressed (d-AoSMC) and non-stressed (AoSMC) VSMCs were collected, and small extracellular vesicles (sEVs) were isolated and pooled (d-AoSMC_Exo and AoSMC_Exo) for cargo analysis by qPCR focused on osteocyte gene markers. Briefly, the sEV were harvested in TRIzol to allow cDNA preparation. Osteocyte gene markers evaluated were, as follows: DMP1 **(a)**, SOST **(b)**, miR-23a **(c)**, and FGF23 **(d)**. In addition, sEV gene markers were newly investigated: CD9 **(e)**, CD63 **(f)**, CD81 **(g)**, and SMPD3 **(h)**. The graphs represent the analysis of 3 independent replicates. qPCR data were normalized using GADPH as a housekeeping gene, and miR-17 was used for normalizing the data of miR-23a expression. Finally, the isolated vesicles **(i)** or those in culture medium **(j)** were used for SOST quantification by ELISA assay. Statistics: $\&p < 0.05$; $\&\&p < 0.1906$, $\&\&\&p < 0.0002$; $\&\&\&\&p < 0.0001$: Statistical difference when comparing shear-stressed (d-AoSMC) and non-stressed (AoSMC) VSMCs-released sEV. Note: $n = 3$ independent biological replicates. Each condition was analyzed in technical triplicate, and the technical triplicates corresponding to each biological replicate were pooled prior to performing the PCR reaction.

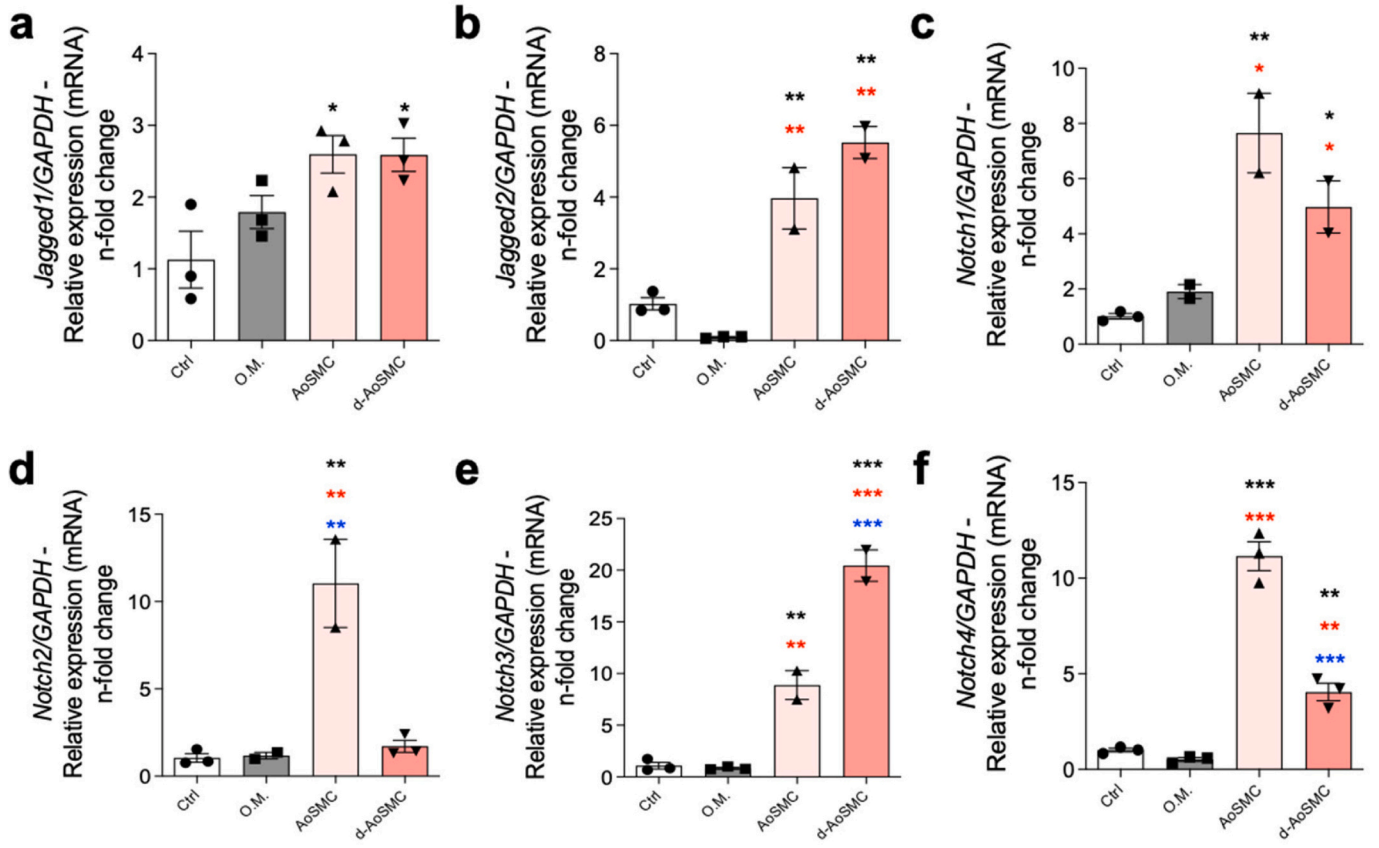


**Fig. 9. VSMC-conditioned medium reprograms Notch signaling–related genes in differentiated osteocytes.** After 28 days of exposure to conditioned media from shear-stressed (d-AoSMC) or non-stressed (AoSMC) VSMCs, cells were harvested in TRIzol for mRNA extraction. Genes related to Notch signaling were duly chosen to be evaluated, as follows: Jagged1 **(a)**, Jagged2 **(b)**, Notch1 **(c)**, Notch2 **(d)**, Notch3 **(e)**, and Notch4 **(f)**. The effect of VSMCs on osteoblasts was compared with control groups: Ctrl – where the cultures were maintained in routine condition, and O.M. – where the cultures were maintained responding to classical chemical osteostimulation medium. The graphs bring the analysis of 3 independent replicates. qPCR data were normalized using GADPH as a housekeeping gene. Statistics: $*p < 0.05$; $**p < 0.1906$, $***p < 0.0002$: Significant statistical difference when compared to Ctrl. *p < 0.05; **p < 0.1906, ***p < 0.0002: Statistical difference when compared with the O.M.. **p < 0.1906; ***p < 0.0002: Statistical difference when comparing osteoblasts cultures responding to shear-stressed (d-AoSMC) and non-stressed (AoSMC) VSMCs. Note: $n = 3$ independent biological replicates. Each condition was analyzed in technical triplicate, and the technical triplicates corresponding to each biological replicate were pooled prior to performing the PCR reaction.

treated with medium enriched with vesicles at a 1:10 ratio. The vesicles were isolated using the Total Exosome Isolation Kit (from cell culture media; 4,478,359, Invitrogen – Thermo Fisher Scientific, Vilnius, Lithuania), following the manufacturer's instructions.

### 4.4. Shear-stress and conditioned medium harvesting

The cells were cultured in appropriate cell culture medium until they reached semi-confluence (90 %), in culture plates 100, prepared by sterilization under UV light for 15 min. Then the medium was replaced with DMEM medium supplemented with 1 % antibiotic and 1 % FBS. The semi-confluent layers were subjected to *Shear-Stress* (using orbital shaker) for 72 h under a humid atmosphere with 5 % $CO_2$ at 37 °C, as previously described by Rodríguez and González, de la Paz et al. The rotation was determined using the maximum stress formula: $\tau max = a\sqrt{\rho\eta(2\pi f)3}$ so that the rotation frequency is within the physiological arterial pressure (6–40_dynes/cm), mimicking the mechanical forces encountered by blood flow [37–39]. At the end, conditioned medium was collected, centrifuged and stored for further analysis. As a control the medium used was conditioned by cells that were maintained static (no rotation; unmechanical-stressed cells) during the culture, under the same culture conditions.

### 4.5. Osteogenic differentiation

For induction of osteoblast differentiation, we treated Osteoblasts with conventional medium in the control group and Bovine Fetal Serum reduced to 1 %. As a positive control, we used classical methodology in the differentiation literature, where β-Glycerophosphate (10 mM) + Dexamethasone (0,03 g/mL) + Ascorbic Acid (50 μg/mL), components purchased together with Sigma- Aldrich. Additional groups were tested, where osteoblasts were treated with conditioned medium by VSMCs subjected or not to Shear-Stress. The cells were kept into the incubator for 28 days, the respective medium being exchanged every 3 days to maintain the biological properties of the study.

### 4.6. Matrix metalloproteinase activities

Osteoblast cultures were treated as detailed previously when the conditioned medium was harvested. The gelatinolytic activities of the samples were evaluated by resolving the sample from cell culture supernatants into SDS-PAGE containing 0.1 % gelatin and 10 % polyacrylamide. Samples, pre-mixed with loading buffer (2 % SDS and 0.1 % bromophenol blue), were electrophoresed. After electrophoresis, the gels were washed in 2 % Triton X-100 and immersed in 50 mM Tris-HCl buffer (pH 7.6), 200 mM NaCl and 10 mM $CaCl_2$ for 18 h at 37 °C. (1:4:5 vol/vol/vol) and decolorized with acetic acid/methanol/water (1:2:7 vol.) were mixed with 0.5 % Coomassie Blue G-250 in acetic acid

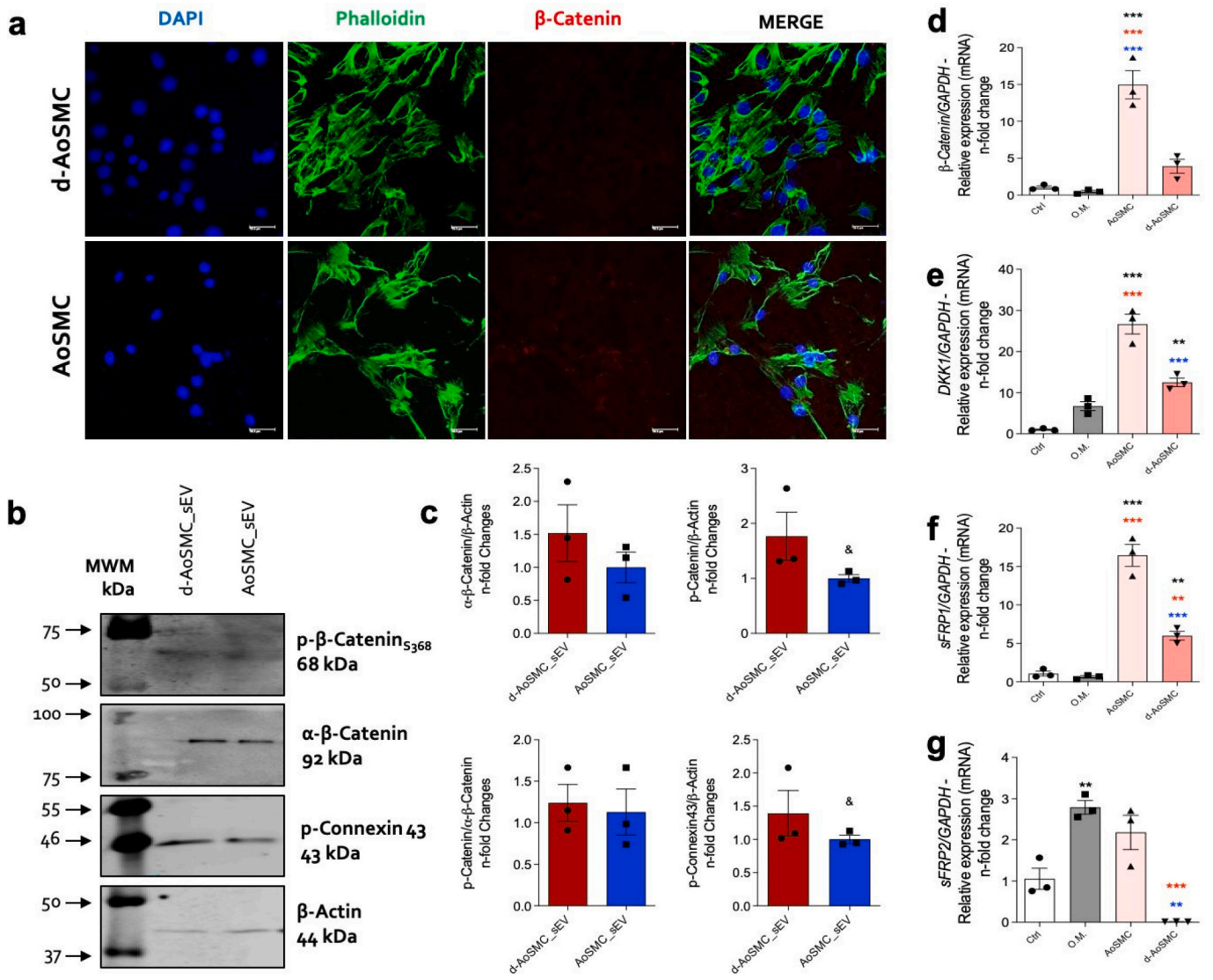


**Fig. 10. β-Catenin appears to be a constitutive signaling pathway in differentiated osteocytes.** VSMCs were grown on coverslips, and after 72 h under each experimental condition (shear-stressed, d-AoSMC; and non-stressed, AoSMC), they were fixed and labeled for β-Catenin to allow image acquisition using laser fluorescent microscopy **(a)**. Moreover, the conditioned media was collected, and the EVs pooled to analyze the presence of p-β-Catenin, β-Catenin, and p-Connexin43 using western blotting **(b)**, with β-Actin serving as the loading control. Densitometry analysis is shown in **(c)**. Finally, we investigated the expression profile of bone cells treated with conditioned media from vascular smooth muscle cells (VSMCs) subjected or not to shear stress. The cells were harvested in TRIzol for subsequent transcript analysis by qPCR, as follows: β-Catenin **(d)**, DKK1 **(e)**, sFRP1 **(f)**, and sFRP2 **(g)**. The graphs bring the analysis of 3 independent replicates. q-PCR data were normalized using GADPH as a housekeeping gene. Statistics: $\&p < 0.05$: Statistical difference when compared shear-stressed (d-AoSMC) and non-stressed (AoSMC) released sEV. $^{**}p < 0.1906$, $^{***}p < 0.0002$: Significant statistical difference when compared to Ctrl. $^{**}p < 0.1906$, $^{***}p < 0.0002$: Statistical difference when compared with the O.M.. $^{**}p < 0.1906$; $^{***}p < 0.0002$: Statistical difference when comparing osteoblasts cultures responding to shear-stressed (d-AoSMC) and non-stressed (AoSMC) VSMCs. Note: $n = 3$ independent biological replicates. Each condition was analyzed in technical triplicate, and the technical triplicates corresponding to each biological replicate were pooled prior to performing the PCR reaction. Immunoblotting: No band splicing was performed. Bands were cropped solely for clarity, with adequate space preserved above and below each signal and the corresponding molecular weight marker. Full, uncropped blots from the same acquisition are provided in the Supplementary Material.

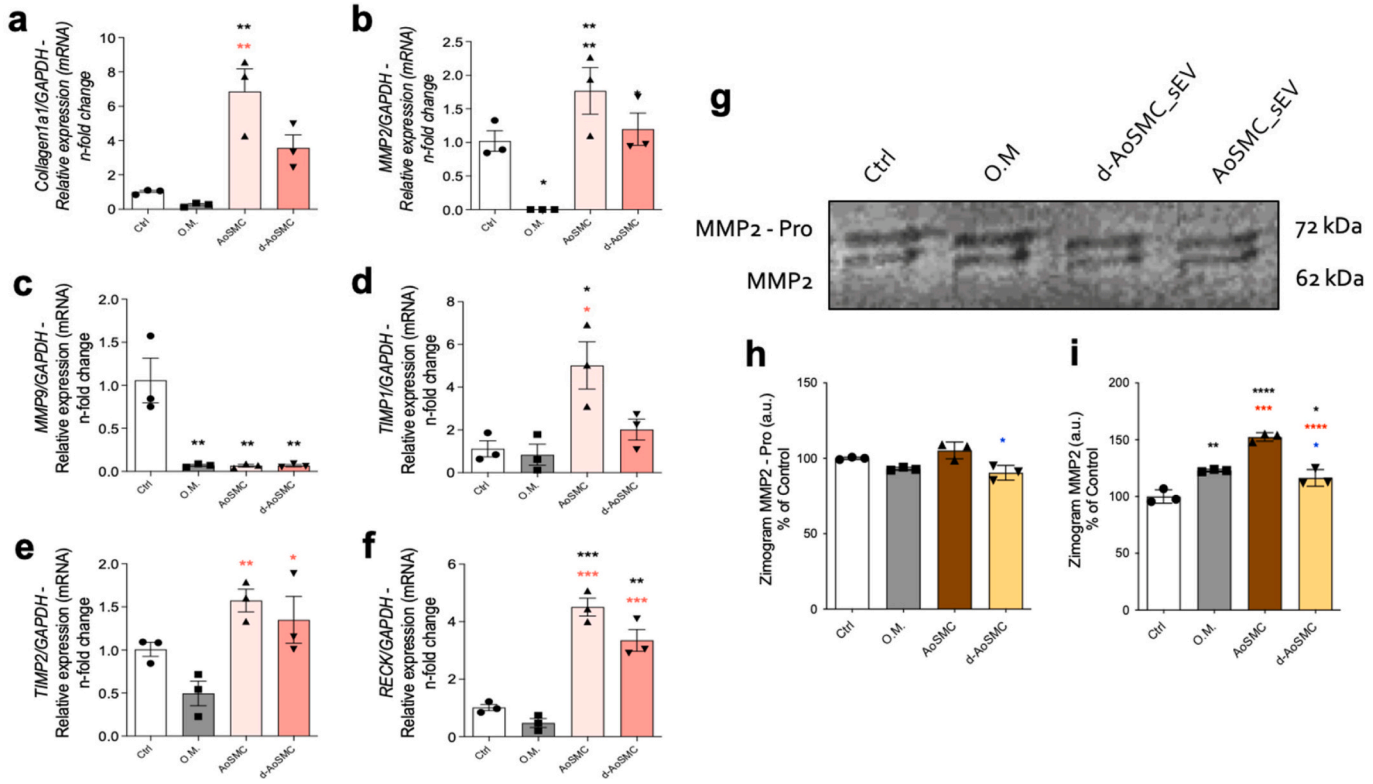


**Fig. 11. Possible osteoid matrix remodeling requires MMP involvement in differentiated osteocytes in vitro.** Thereafter 28 days in culture responding to shear-stressed (d-AoSMC) and non-stressed (AoSMC) VSMCs conditioned media, the cells were harvested in TRIzol to allow mRNA extraction, and the conditioned media collected for further investigating MMP activities performing zymography. ECM remodeling-related genes were duly chosen to be evaluated, as follows: Col1a1 **(a)**, MMP2 **(b)**, MMP9 **(c)**, TIMP1 **(d)**, TIMP2 **(e)**, and RECK **(f)**. Briefly, the conditioned media were properly prepared and resolved in an electrophoresis gel containing gelatin (substrate for gelatinase), and the activity of MMP2 was identified **(g)**, and the densitometry analysis is shown considering proMMP2 **(h)**, and active MMP2 **(i)**. The effect of VSMCs on osteoblasts was compared with control groups: Ctrl – where the cultures were maintained in routine condition, and O.M. – where the cultures were maintained responding to classical chemical osteostimulation medium. The graphs bring the analysis of 3 independent replicates. qPCR data were normalized using GADPH as a housekeeping gene. Statistics: $*p < 0.05$; $**p < 0.1906$, $***p < 0.0002$: Significant statistical difference when compared to Ctrl. $*p < 0.05$; $**p < 0.1906$, $***p < 0.0002$; $****p < 0.0001$: Statistical difference when compared with the O.M.. $*p < 0.05$: Statistical difference when compared osteoblasts cultures responding to shear-stressed (d-AoSMC) and non-stressed (AoSMC) VSMCs. Note: $n = 3$ independent biological replicates. Each condition was analyzed in technical triplicate, and the technical triplicates corresponding to each biological replicate were pooled prior to performing the PCR reaction.

[40,41].

### 4.7. Sample preparation and qPCR analysis

For collection of samples for qPCR, after 28 days of treatment the TriZOL (500 μL) was added. Total mRNA samples were quantitated using microplate reader (SYNERGY-HTX multi-mode reader, Biotek, USA). The cDNA synthesis using the High-Capacity cDNA Reverse Transcription Kit. Applied Biosystems (2.0 μL of 10 X RT Buffer, 0.8 μL 25 X dNTP Mix (100 mM), 2.0 μL 10 X RT Randon Primers, 1.0 μL MultiScribleTM Reverse Transcriptase, 4.2 μL Nuclease- Free $H_2O$). After this process the material was collected and sample was stored in −80 °C freezer. Reaction condition: 95 °C - 15 s; 60 °C - 30s; 72 °C - 30s.

### 4.8. Confocal laser microscopy

For confocal microscopy analysis, the cells were cultured in glass coverslips placed in the peripheral ring of the culture and subjected to Shear-Stress and Static. The cells were then washed with PBS, fixed in PBS-paraformaldehyde (4 % *v*/v), permeabilized in PBS containing 0.2 % Triton-X 100 and 1 % BSA at 37 °C for 1 h stained with the appropriate specific primary antibodies, at the concentration recommended by the manufacturer. Then, after washing with PBS to remove the primary antibody, for fluorescence analysis, cells were stained with anti-rabbit or mouse IgA Alexa Fluor 594 antibody for 1 h. For actin cytoskeletal rearrangement analyzes, the cells were incubated for 40 min at 4 mg/ml, Alexa Fluor 488-labeled phalloidin (Invitrogen/Molecular Probes, USA). Cells were washed and mounted on glass slides using Fluoroshield with DAPI (Sigma) and then viewed on an inverted laser scanning confocal microscope (Leica TCS SP5).

### 4.9. Isolation of small extracellular vesicles (sEV)

For the analysis of sEV, the culture medium was supplemented with extracellular vesicles derived from Free Fetal Serum. The extraction was performed using ultracentrifugation at 30,000 ×*g* for 18 h [42]. After this process, the cells were maintained for 72 h in EV-free, Static, or Shear-Stress conditions. Subsequently, the culture medium was removed and used to isolate sEV with the Total Exosome Isolation Kit (from cell culture media; 4,478,359, Invitrogen - Thermo Fisher Scientific, Vilnius, Lithuania), following the manufacturer's instructions.

### 4.10. Nanoparticle screening (NTA)

NanoSight NS300 (Amesbury, UK) was used to determine the size and concentration of sEV. After isolation of the EVs from the culture medium the sEV were resuspended in PBS for analysis. In all analyzes the samples were diluted 1:1000 in PBS filtered in a 0.22 μm pore filter. Each experiment was performed at 25 °C in triplicate with acquisition of five 1-min videos. The values of concentration, mean size and particle distribution (D10, D50 and D90) were obtained in each of the experiments using the corresponding software (NanoSight software version

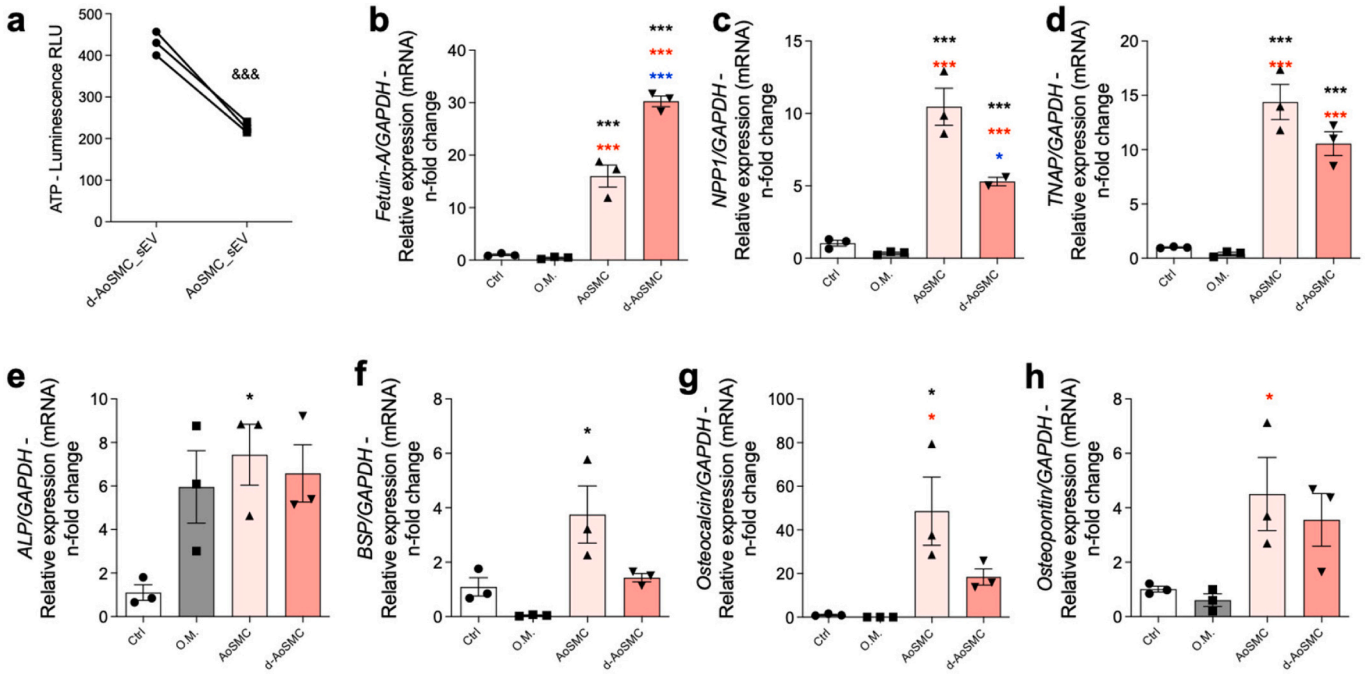


**Fig. 12. VSMC-derived sEVs carry ATP and drive osteocyte mineralization.** sEV were pooled from the conditioned media by VSMCs subjected to the mechanosignaling program [shear-stressed (d-AoSMC) and non-stressed (AoSMC)]. The sEV cargo was investigated, and our data show their capacity to carry ATP **(a)**, with a differential behavior under mechanosignaling stimulus. Thereafter, differentiated osteocytes were analyzed considering genes related to mineralization, such as Fetuin-A **(b)**, NPP1 **(c)**, TNAP **(d)**, ALP **(e)**, BSP **(f)**, osteocalcin **(g)**, and osteopontin **(h)**. The effect of VSMCs on osteoblasts was compared with control groups: Ctrl – where the cultures were maintained in routine condition, and O.M. – where the cultures were maintained responding to classical chemical osteostimulation medium. The graphs bring the analysis of 3 independent replicates. qPCR data were normalized using GADPH as a housekeeping gene. Statistics: &&&$p < 0.0002$: Statistical difference when compared shear-stressed (d-AoSMC) and non-stressed (AoSMC) released sEV. *$p < 0.05$; **$p < 0.1906$, ***$p < 0.0002$: Significant statistical difference when compared to Ctrl. *$p < 0.05$; **$p < 0.1906$, ***$p < 0.0002$: Statistical difference when compared with the O.M.. *$p < 0.05$; **$p < 0.1906$; ***$p < 0.0002$: Statistical difference when compared osteoblasts cultures responding to shear-stressed (d-AoSMC) and non-stressed (AoSMC) VSMCs. Note: $n = 3$ independent biological replicates. Each condition was analyzed in technical triplicate, and the technical triplicates corresponding to each biological replicate were pooled prior to performing the PCR reaction.

2.3).

### 4.11. Zeta potential A

The Malvern Zetasizer Nano ZS instrument was used to measure zeta potential. sEV were first diluted 100 times in PBS and pH was adjusted to neutral pH (7.4–7.7) with standard NaOH (0.1 N). Samples were then loaded into a pre-rinsed folded capillary cell, and measurements were taken at 25 °C for all samples using an applied voltage of 150 V of three measurements were made for each sample.

### 4.12. Transmission electron microscopy

For Transmission Microscopy analysis, the sEV were added to the forked coated nickel cadmium for 2 h. After this period the grid was washed in PBS and the material was fixed in 2 % paraformaldehyde for 15 min. Then the grades were washed again with PBS and treated with 2.5 % glutaraldehyde fixative powder for 10 min. The material was washed in deionized water and contrasted with 2 % uranyl acetate for 15 min. Finally, the sample was incubated with 0.13 % methylcellulose and 0.4 % uranyl acetate for 10 min. The excess liquid was removed and after drying the material was analyzed in Fei Company's Tecnai Spirit Electronic Transmission Microscope.

### 4.13. Analysis of small extracellular vesicles markers by flow cytometry

After isolation the sEV were coupled to Latex Beads (ThermoFisher) overnight [42]. The next day the samples were centrifuged and washed with 1 M Glycine. The sEV were distributed in tubes for cytometry and incubated with BD Biosciences antibodies, with respective fluorochromes: anti-CD9, anti-CD63 and anti-CD81 for 30 min in the dark. Thereafter, they were centrifuged at 400 *g* for 5 min and the pellet resuspended in PBS. For the design of the standards, the control tubes were incubated with isotype antibodies specific for each fluorochrome in each test performed. Measurements, 10,000 events for each sample were required on a FACSCantoTM II flow cytometer (BD Biosciences) with FACSDIVA software (BD Biosciences). The results were analyzed in FLOWJO software, version vX.10 × 6 (FlowJo, LLC, Ashland, OR).

### 4.14. ATP assay

For ATP dosing the sEV were boiled at 45 °C for 2 min and dosing was performed according to the instructions of the CellTiter-Glo® Luminescent Cell Viability Assay Technical Bulletin Kit (Promega, Madison, Wisconsin, USA).

### 4.15. Quantification of sclerostin

Extracelular vesicles or conditioned medium Sclerostin (SOST) concentrations were determined by sandwich ELISA using the Human Sclerostin ELISA kit (Thermo Fisher Scientific, USA), following the manufacturer's instructions. Assays were performed with sequential incubation of samples, biotinylated conjugate, and streptavidin-HRP, followed by development with TMB substrate. Absorbance was measured at 450 nm, and concentrations were calculated by interpolation from a standard curve, taking the dilution factor into account.

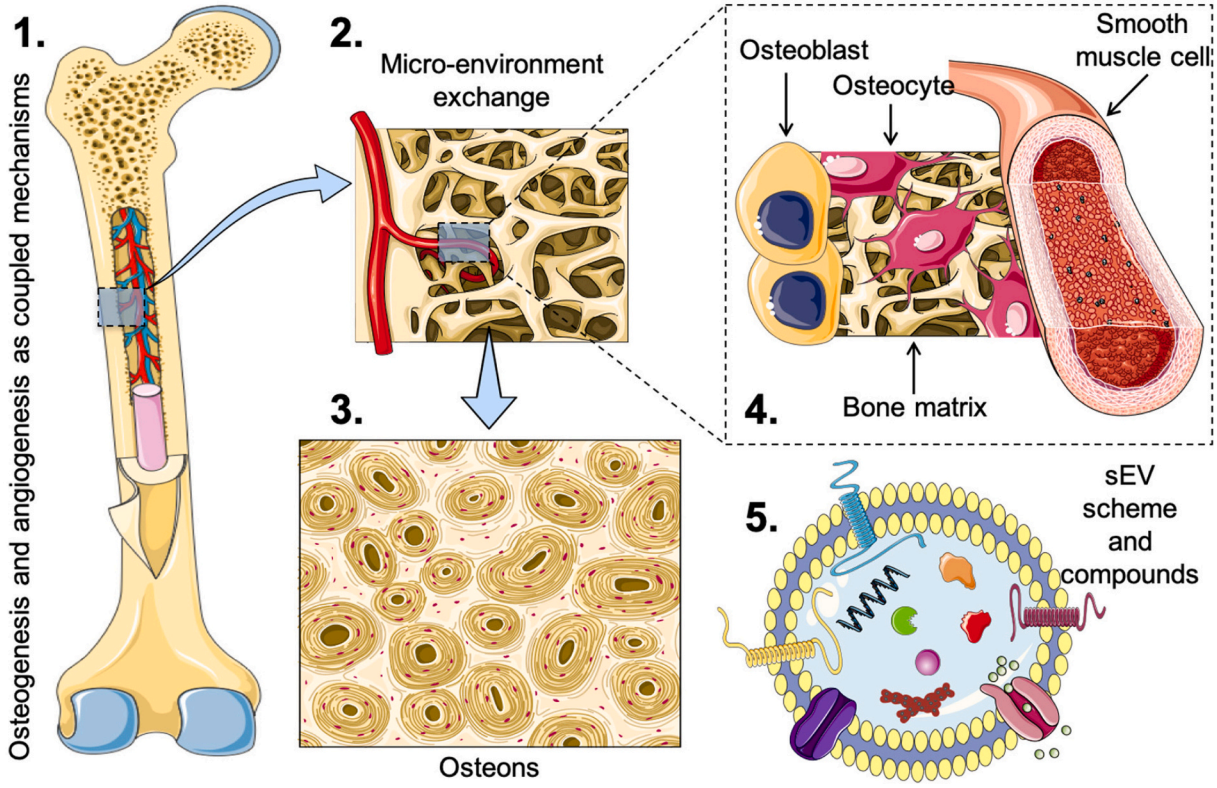


**Fig. 13.** Schematic representation of the interaction between the vascular system and bone tissue, highlighting the role of vascular smooth muscle cells (VSMCs) in osteoblastic differentiation and the osteoblast-to-osteocyte transition. Bone vascularization **(1)** and its proximity to the mineralized matrix illustrate the microenvironment in which osteoblasts undergo phenotypic changes until becoming osteocytes **(2–4)**. The interface between bone marrow, mesenchymal stromal cells (MSCs), VSMCs, and trabecular matrix is shown **(4)**, where paracrine signals modulate osteogenic commitment. In detail, a small extracellular vesicle (sEV) containing RNAs, signaling proteins, and bioactive molecules is presented as an essential mediator of this cell-to-cell communication **(5)**. These VSMC-derived vesicles, particularly under quiescent conditions, promote the activation of osteogenic and osteocytic pathways (including SOST, DMP1, FGF23, and miR-23a), enhancing osteocytic function independently of direct mechanical stimuli and reinforcing the existence of a specific vascular–skeletal communication axis.

### *4.16. Western blotting*

Isolated sEV were lysed on ice for 2 h with Lysis Cocktail (Tris [tris (hydroxymethyl) aminomethane] -HCl [pH 7.4], 1 % Tween 20, 0.25 % sodium deoxycholate, 150 mM NaCl, 1 mM EGTA (ethylene glycol tetracetic acid), 1 mM O-Vanadate, 1 mM NaF and protease inhibitors [1 μg/mL aprotinin, 10 μg/mL leucine, and 1 mM 4- (2-amino -ethyl) -benzolsulfonyl-fluoro-hydrochloride]). After being lysed, the samples were sonicated (1 pulse per second; SONICS Vibra-Cell, USA). The protein extracts were clarified and the protein concentration determined by the Lowry method [42,43]. Protein extracts were resolved by SDS-PAGE (12 %) and transferred to PVDF membranes (Bio-Rad, Hercules, CA, USA). Immediately, the membranes were blocked with bovine serum albumin (2.5 %) in Tris buffered saline (TBS) -20 (0.05 %) and incubated overnight at 4 °C with appropriate primary antibody. After washing in TBS-Tween 20 (0.05 %), the membranes were incubated with secondary antibodies conjugates for 1 h. Subsequently, Enhancement Chemiluminescence (ECL, Pierce, USA) was used to detect the bands. Importantly, no band splicing was performed. Bands were cropped solely for clarity, preserving adequate space above and below each signal and the corresponding molecular weight marker on the right side of the blot. Full, uncropped blots from the same acquisition are provided in the Supplementary Material.

### *4.17. Statistical analysis*

All experiments were performed in triplicate (independent replicates) and the data expressed as the mean ± standard deviation (SD). They were verified using One-Way ANOVA with Tukey's post-test to compare all pairs of groups (where $p < 0.05$ was considered statistically significant; $p < 0.0001$ highly significant). The software used was GraphPad Prism 6. ImageJ Software was used for vesicles and osteocytes counting. For the statistical analysis, qPCR data were standardized considering fold changes of the control.

## CRediT authorship contribution statement

**Célio J.C. Fernandes:** Writing – review & editing, Writing – original draft, Software, Methodology, Investigation, Formal analysis, Data curation. **Bram C.J. van der Eerden:** Writing – review & editing, Writing – original draft, Validation, Software, Methodology, Formal analysis. **Rodrigo A. Foganholi Silva:** Writing – review & editing, Writing – original draft, Methodology, Investigation, Formal analysis, Data curation. **Gwenny M. Fuhler:** Writing – review & editing, Writing – original draft, Investigation, Formal analysis, Data curation. **Maikel P. Peppelenbosch:** Writing – review & editing, Writing – original draft, Validation, Supervision, Conceptualization. **Willian F. Zambuzzi:** Writing – review & editing, Writing – original draft, Supervision, Project administration, Funding acquisition, Conceptualization.

## Declaration of competing interest

The authors declare that they have no known competing financial interests or personal relationships that could have appeared to influence the work reported in this paper.

## Acknowledgements

The authors are grateful to Fundação de Amparo à Pesquisa do Estado de São Paulo (FAPESP), grants numbers: 2014/22689-3; 2016/08888-9; 2019/21807-6; 2018/10856-3 and CNPq.

## Appendix A. Supplementary data

Supplementary data to this article can be found online at https://doi.org/10.1016/j.bbamcr.2025.120092.

## Data availability

Data will be made available on request.

## References

[1] A.P. Kusumbe, S.K. Ramasamy, R.H. Adams, Erratum: corrigendum: coupling of angiogenesis and osteogenesis by a specific vessel subtype in bone, Nature 513 (2014) 574.
[2] A.P. Kusumbe, R.H. Adams, Osteoclast progenitors promote bone vascularization and osteogenesis, Nat. Med. 20 (2014) 1238–1240.
[3] S.G. Romeo, K.M. Alawi, J. Rodrigues, A. Singh, A.P. Kusumbe, S.K. Ramasamy, Endothelial proteolytic activity and interaction with non-resorbing osteoclasts mediate bone elongation, Nat. Cell Biol. 21 (2019) 430–441.
[4] Y.-Q. Yang, Y.-Y. Tan, R. Wong, A. Wenden, L.-K. Zhang, A.B.M. Rabie, The role of vascular endothelial growth factor in ossification, Int. J. Oral Sci. 4 (2012) 64–68.
[5] B. Beamer, C. Hettrich, J. Lane, Vascular endothelial growth factor: an essential component of angiogenesis and fracture healing, HSS J. 6 (2010) 85–94.
[6] S.K. Ramasamy, A.P. Kusumbe, R.H. Adams, Regulation of tissue morphogenesis by endothelial cell-derived signals, Trends Cell Biol. 25 (2015) 148–157.
[7] K.K. Sivaraj, R.H. Adams, Blood vessel formation and function in bone, Development 143 (2016) 2706–2715.
[8] S.K. Ramasamy, A.P. Kusumbe, M. Schiller, D. Zeuschner, M.G. Bixel, C. Milia, J. Gamrekelashvili, A. Limbourg, A. Medvinsky, M.M. Santoro, F.P. Limbourg, R. H. Adams, Blood flow controls bone vascular function and osteogenesis, Nat. Commun. 7 (2016) 13601.
[9] U. Saran, S. Gemini Piperni, S. Chatterjee, Role of angiogenesis in bone repair, Arch. Biochem. Biophys. 561 (2014) 109–117.
[10] K. Zhang, C. Barragan-Adjemian, L. Ye, S. Kotha, M. Dallas, Y. Lu, S. Zhao, M. Harris, S.E. Harris, J.Q. Feng, L.F. Bonewald, E11/gp38 selective expression in osteocytes: regulation by mechanical strain and role in dendrite elongation, Mol. Cell. Biol. 26 (2006) 4539–4552.
[11] P. Kuczera, M. Adamczak, A. Wiecek, Fibroblast growth Factor-23—a potential uremic toxin, Toxins (Basel) 8 (2016) 369.
[12] A. Sakurai, T. Hasegawa, A. Kudo, Z. Shen, T. Nagai, M. Abe, T. Yoshida, H. Hongo, T. Yamamoto, T. Yamamoto, K. Oda, P.H.L. de Freitas, M. Li, H. Sano, N. Amizuka, Chronological immunolocalization of sclerostin and FGF23 in the mouse metaphyseal trabecular and cortical bone, Biomed. Res. 38 (2017) 257–267.
[13] H. Yamamoto, B. Ramos-Molina, A.N. Lick, M. Prideaux, V. Albornoz, L. Bonewald, I. Lindberg, Posttranslational processing of FGF23 in osteocytes during the osteoblast to osteocyte transition, Bone 84 (2016) 120–130.
[14] D. Mattinzoli, M.P. Rastaldi, M. Ikehata, S. Armelloni, C. Pignatari, L.A. Giardino, M. Li, C.M. Alfieri, A. Regalia, D. Riccardi, P. Messa, FGF23-regulated production of Fetuin-a (AHSG) in osteocytes, Bone 83 (2016) 35–47.
[15] L.F. Bonewald, The amazing osteocyte, J. Bone Miner. Res. 26 (2011) 229–238.
[16] M.C. Bezerra, J.F. Carvalho, A.S. Prokopowitsch, R.M.R. Pereira, RANK, RANKL and osteoprotegerin in arthritic bone loss, Braz. J. Med. Biol. Res. 38 (2005) 161–170.
[17] C. Davenport, E. Harper, H. Forde, K.D. Rochfort, R.P. Murphy, D. Smith, P. M. Cummins, RANKL promotes osteoblastic activity in vascular smooth muscle cells by upregulating endothelial BMP-2 release, Int. J. Biochem. Cell Biol. 77 (2016) 171–180.
[18] K.M. Shah, P. Orton, N. Mani, J.M. Wilkinson, A. Gartland, Osteocyte physiology and response to fluid shear stress are impaired following exposure to cobalt and chromium: implications for bone health following joint replacement, J. Orthop. Res. 35 (2017) 1716–1723.
[19] R.F.M. van Oers, H. Wang, R.G. Bacabac, Osteocyte shape and mechanical loading, Curr. Osteoporos. Rep. 13 (2015) 61–66.
[20] S.L. Dallas, M. Prideaux, L.F. Bonewald, The osteocyte: an endocrine cell … and more, Endocr. Rev. 34 (2013) 658–690.
[21] I. Kramer, C. Halleux, H. Keller, M. Pegurri, J.H. Gooi, P.B. Weber, J.Q. Feng, L. F. Bonewald, M. Kneissel, Osteocyte Wnt/β-catenin signaling is required for Normal bone homeostasis, Mol. Cell. Biol. 30 (2010) 3071–3085.
[22] J. Xiong, M. Onal, R.L. Jilka, R.S. Weinstein, S.C. Manolagas, C.A. O'Brien, Matrix-embedded cells control osteoclast formation, Nat. Med. 17 (2011) 1235–1241.
[23] H. Takayanagi, RANKL as the master regulator of osteoclast differentiation, J. Bone Miner. Metab. 39 (2021) 13–18.
[24] M. Asagiri, H. Takayanagi, The molecular understanding of osteoclast differentiation, Bone 40 (2007) 251–264.
[25] C.J.C. Fernandes, R.A. Silva, M.R. Ferreira, G.M. Fuhler, M.P. Peppelenbosch, B.C. J. van der Eerden, W.F. Zambuzzi, Vascular smooth muscle cell-derived exosomes promote osteoblast-to-osteocyte transition via β-catenin signaling, Exp. Cell Res. 442 (2024) 114211.
[26] S. Zhu, W. Chen, A. Masson, Y.-P. Li, Cell signaling and transcriptional regulation of osteoblast lineage commitment, differentiation, bone formation, and homeostasis, Cell Discov. 10 (2024) 71.
[27] A. Marahleh, H. Kitaura, F. Ohori, T. Noguchi, I. Mizoguchi, The osteocyte and its osteoclastogenic potential, Front. Endocrinol. (Lausanne) 14 (2023).
[28] H.-C. Zeng, Y. Bae, B.C. Dawson, Y. Chen, T. Bertin, E. Munivez, P.M. Campeau, J. Tao, R. Chen, B.H. Lee, MicroRNA miR-23a cluster promotes osteocyte differentiation by regulating TGF-β signalling in osteoblasts, Nat. Commun. 8 (2017) 15000.
[29] R.R. Gupta, D.J. Yoo, C. Hebert, C. Niger, J.P. Stains, Induction of an osteocyte-like phenotype by fibroblast growth factor-2, Biochem. Biophys. Res. Commun. 402 (2010) 258–264.
[30] R. Nishimura, Y. Kato, D. Chen, S.E. Harris, G.R. Mundy, T. Yoneda, Smad5 and DPC4 are key molecules in mediating BMP-2-induced osteoblastic differentiation of the pluripotent mesenchymal precursor cell line C2C12, J. Biol. Chem. 273 (1998) 1872–1879.
[31] K.K. Sivaraj, R.H. Adams, Blood vessel formation and function in bone, Development 143 (2016) 2706–2715.
[32] K.K. Sivaraj, R.H. Adams, Blood vessel formation and function in bone, Development 143 (2016) 2706–2715.
[33] C.J.C. Fernandes, R.A. Silva, M.R. Ferreira, G.M. Fuhler, M.P. Peppelenbosch, B.C. J. van der Eerden, W.F. Zambuzzi, Vascular smooth muscle cell-derived exosomes promote osteoblast-to-osteocyte transition via β-catenin signaling, Exp. Cell Res. 442 (2024) 114211.
[34] C.M. Gordon, L.B. Gordon, B.D. Snyder, A. Nazarian, N. Quinn, S. Huh, A. Giobbie-Hurder, D. Neuberg, R. Cleveland, M. Kleinman, D.T. Miller, M.W. Kieran, Hutchinson-gilford progeria is a skeletal dysplasia, J. Bone Miner. Res. 26 (2011) 1670–1679.
[35] J.A. Welsh, D.C.I. Goberdhan, L. O'Driscoll, E.I. Buzas, C. Blenkiron, B. Bussolati, H. Cai, D. Di Vizio, T.A.P. Driedonks, U. Erdbrügger, J.M. Falcon-Perez, Q. Fu, A. F. Hill, M. Lenassi, S.K. Lim, M.G. Mahoney, S. Mohanty, A. Möller, R. Nieuwland, T. Ochiya, et al., Minimal information for studies of extracellular vesicles (MISEV2023): from basic to advanced approaches, J. Extracell. Vesicles 13 (2024).
[36] C.J. da Costa Fernandes, W.F. Zambuzzi, Fibroblast-secreted trophic factors contribute with ECM remodeling stimulus and upmodulate osteocyte gene markers in osteoblasts, Biochimie 168 (2020) 92–99.
[37] N.G. dela Paz, T.E. Walshe, L.L. Leach, M. Saint-Geniez, P.A. D'Amore, Role of shear-stress-induced VEGF expression in endothelial cell survival, J. Cell Sci. 125 (2012) 831–843.
[38] R.A. da Silva, A.F. de Camargo Andrade, G. da Silva Feltran, C.J. da C. Fernandes, R.I.F. de Assis, M.R. Ferreira, D.C. Andia, W.F. Zambuzzi, The role of triiodothyronine hormone and mechanically-stressed endothelial cell paracrine signalling synergism in gene reprogramming during hBMSC-stimulated osteogenic phenotype in vitro, Mol. Cell. Endocrinol. 478 (2018) 151–167.
[39] R.A. da Silva, C.J. da C. Fernandes, G. da S. Feltran, A.M. Gomes, A.F. de Camargo Andrade, D.C. Andia, M.P. Peppelenbosch, W.F. Zambuzzi, Laminar shear stress-provoked cytoskeletal changes are mediated by epigenetic reprogramming of TIMP1 in human primary smooth muscle cells, J. Cell. Physiol. 234 (2019) 6382–6396.
[40] V. Lefebvre, C. Peeters-Joris, G. Vaes, Production of gelatin-degrading matrix metalloproteinases ('type IV collagenases') and inhibitors by articular chondrocytes during their dedifferentiation by serial subcultures and under stimulation by interleukin-1 and tumor necrosis factor alpha, Biochim. Biophys. Acta 1094 (1991) 8–18.
[41] V. Lefebvre, C. Peeters-Joris, G. Vaes, Production of gelatin-degrading matrix metalloproteinases ('type IV collagenases') and inhibitors by articular chondrocytes during their dedifferentiation by serial subcultures and under stimulation by interleukin-1 and tumor necrosis factor α, Biochim. Biophys. Acta (BBA) – Mol. Cell Res. 1094 (1991) 8–18.
[42] A. Mehdiani, A. Maier, A. Pinto, M. Barth, P. Akhyari, A. Lichtenberg, An innovative method for exosome quantification and size measurement, J. Vis. Exp. (2015).
[43] E.F. Hartree, Determination of protein: a modification of the Lowry method that gives a linear photometric response, Anal. Biochem. 48 (1972) 422–427.
[44] G. da Silva Feltran, R. Augusto da Silva, C.J. da Costa Fernandes, M.R. Ferreira, Dos Santos SAA, L.A. Justulin Junior, L. Del Valle Sosa, W.F. Zambuzzi, Vascular smooth muscle cells exhibit elevated hypoxia-inducible factor-1α expression in human blood vessel organoids, influencing osteogenic performance, Exp. Cell Res. 440 (2) (2024 Jul 15) 114136, https://doi.org/10.1016/j.yexcr.2024.114136 (Epub 2024 Jun 22. PMID: 38909881).